Neuroscience

Input-specific gating of NMDA amplification via HCN channels in mouse L2/3 pyramidal neurons

Viktor János Oláh, Jing Wu, Leonard K Kaczmarek, Matthew JM Rowan

Department of Cell Biology, Emory University School of Medicine, Atlanta, United States • Department of Pharmacology, Yale University School of Medicine, New Haven, United States • Department of Cellular and Molecular Physiology, Yale University School of Medicine, New Haven, United States • Center for Neurodegenerative Disease, Emory University School of Medicine, Atlanta, United States

Reviewed Preprint
v2 • January 15, 2025
Revised by authors

Reviewed Preprint
v1 • April 3, 2024

eLife Assessment

In this **valuable** study the authors use electrophysiology in brain slices and computer modeling and suggest that layer 2/3 pyramidal neurons of the mouse cortex have functional HCN channels on the proximal apical dendrite which allows distinct processing of input at that location from the input to distal apical dendrites. The revisions improved the **solid** paper but some of the concerns were not addressed sufficiently and many of these concerns could be addressed by further revision.

https://doi.org/10.7554/eLife.96002.2.sa3

Abstract

Layer 2/3 pyramidal cells (L2/3 PCs) play a crucial role in cortical information transfer. Although the dendritic arbors of L2/3 PCs are impressive, they often lack the distinct anatomical compartments characteristic of deeper L5 PCs. For example, many L2/3 PCs do not display an apparent distal tuft region. However, L2/3 PCs receive inputs from both thalamic (bottom-up) and cortical (top-down) inputs, which preferentially synapse onto their proximal and distal dendrites, respectively. Nonuniform organization of channels and NMDA receptors in L2/3 dendrites could serve to independently modulate these information streams to affect learning and behavior, yet whether L2/3 PC dendrites possess this capability has not been established. Here we found a previously unappreciated, non-uniform HCN channel distribution in L2/3 PCs, allowing for pathway-specific gating of NMDA receptor recruitment at bottom-up (proximal) but not top-down (distal) synapses. HCN availability shifted depending on developmental stage and neuromodulation, suggesting that the gain of thalamic and cortical-cortical signals in L2/3 may be independently modified *in vivo* across different timescales.

Introduction

Layer 2/3 pyramidal cells (L2/3 PCs) are the most numerous excitatory neurons in the neocortex. As a major component of the canonical circuit, L2/3 PCs are thought to play crucial roles in information transfer and gain control of cortical output(1). Thus, disambiguating the afferent circuit connections of L2/3 PCs has been a significant focus of neuroscience research in the past decade(2–5). However, understanding cellular mechanisms by which L2/3 PCs transform information is equally important (6–9). Like their more extensively studied counterparts (e.g., L5 PT-type PCs, hippocampal CA1 PCs), L2/3 PCs are equipped with an array of dendritic nonlinearities(10, 11), enabling complex subcellular computations. Nonetheless, L2/3 PCs exhibit marked disparities from other PC types as well. Their morphology is less segmented due to the lack of a distinctive apical tuft (except for the deepest layer 3 cells (12)). Their dendritic protrusions are also shorter and consequently possess less surface area over which specialized nonlinear operations may be actualized. Therefore, the applicability of currently established neuronal dynamics to L2/3 PCs is questionable.

Dendritic voltage-gated channels and receptors are crucial for diversifying the computational power of neuronal cells, by allowing for nonlinear processing of arriving synaptic inputs(13). Nonlinear processing is essential for proper brain function and has been implicated in critical tasks such as conscious perception(14–16) and processing of sensory and motor input(17). Therefore, a more comprehensive understanding of subcellular signal processing dynamics in L2/3 PCs is warranted. Dendritic hyperpolarization-activated nonselective cation (HCN) channels are a staple of several PC classes(18, 19), playing essential roles in regulating resting membrane potential, the normalization of synaptic events arriving at spatially mismatched locations, and establishing oscillation frequency-selectivity(16). Beyond exerting control over the general excitability of neurons, HCN channels contribute to synaptic plasticity, and can regulate working memory(16). HCN dysfunction can also contribute to epilepsy and pain(20). Electrophysiological detection of this current often relies on identification of a characteristic ‘sag’ potential, elicited by hyperpolarizing current injections. In L2/3 PCs, this sag potential is negligible in most cortical areas (but see (21)) thus HCN channels are often presumed to be missing from mouse L2/3 PCs (22). However, it has recently been proposed that HCN is a key determinant of L2/3 PC passive properties at membrane potentials close to rest, despite the lack of traditional HCN channel physiological markers (23). In contrast to mice, the presence of HCN channels in L2/3 PCs of primates and humans is unambiguously supported by functional and anatomical evidence as well (24, 25) (26).

Here we report that L2/3 PCs throughout the cortex express functionally relevant HCN channels with unexpected functions. We found that HCN channels robustly influence the overall excitability of L2/3 PCs. Interestingly, we found that HCN channel availability in L2/3 PCs is biased in a unique proximal somato-dendritic manner, which is inverted with respect to L5 PT-type and hippocampal CA1 PCs (but see (27)), where HCN is enriched within their distal apical tufts(19, 28). In cooperation with local NMDA receptors, we found this L2/3 HCN organization could gate the amplification of proximal ‘bottom-up’ dendritic inputs, without affecting distal ‘top-down’ dendritic inputs. Furthermore, we found that HCN expression is robustly upregulated during early postnatal development, and that neuromodulation in adulthood can rapidly adjust HCN channel availability. Our results demonstrate that L2/3 PCs not only express dendritic HCN channels, but also employ these conductances in a previously unappreciated synaptic input-selective manner.

Results

HCN channel expression in L2/3 PCs

HCN channels have been extensively documented and rigorously characterized in several cortical PC types(18), however, whether PCs residing in layer 2/3 of the mouse cortex express functionally relevant HCN channels remains ambiguous. Nonetheless, open-source snRNAseq (29) shows comparable HCN subunit mRNA levels in all cortical PC types of the visual cortex (**Fig. 1a**). Therefore, we investigated whether this mRNA signature translated to HCN surface expression. Immunohistochemical staining against HCN1 showed discernible somatic fluorescent signal in many cells residing in superficial layers of the cortex (**Fig. 1b**) along with staining of putative dendrites. To examine the potential functional role for HCN channels in L2/3 PCs, we performed *ex vivo* cell-attached recordings from visually identified L2/3 PCs in primary visual cortex slices from mature mice. Spike output upon extracellular stimulation (50 Hz) in layer 4 was then measured in control conditions and following pharmacological HCN channel block (**Fig. 1c**). We found that bath application of ZD-7288 (50 µM), a conventional blocker of HCN channels, significantly increased their firing (**Fig. 1d,e**). Similar results were obtained using another well-accepted HCN channel blocker; external Cs^+ (2 mM, **Fig. 1f,g**). This effect was unlikely due to presynaptic modulation of these synapses, as the paired-pulse ratio was unchanged in a set of separate whole-cell recordings coupled with stimulation in layer 4 (**Fig. 1h**). Together, these results indicate that L2/3 PCs express a functionally relevant set of HCN channels which can modulate AP firing following synaptic stimulation.

HCN channels constrain the overall excitability of L2/3 PCs

To investigate the role of HCN channels in regulating the excitability of L2/3 PCs, we performed further L2/3 PC whole-cell recordings. A conventionally used assessment of HCN channel function is the characterization of the sag potential(18). This hallmark of I_h activation is measured as the amount of rectification detected in response to hyperpolarizing current injections. In line with previous reports(30), we found that L2/3 PCs exhibited an unremarkable amount of sag potential at 'typical' current commands. However, upon larger negative current injections, a discernable rectification was revealed (**Fig. 2a**). In addition, the rectification of the steady-state responses was abolished in the presence of external Cs^+, which could be restored by artificial I_h supplementation by dynamic clamp (**Fig. 2b**). Similarly, sag became non-detectable when I_h was blocked, which could then be online restored during recordings by dynamic clamp (**Fig. 2c,d**). Furthermore, we found that passive electrical properties were also significantly modulated by HCN blockade (**Fig. 2e,f**, **Supplementary Fig. 1**), however, action potential halfwidth was unaffected (1.04 ± 0.09 ms vs. 1.12 ± 0.17 ms for control vs. CsMeSO4 bath application; p=0.324, t(6)=-1.073, Student's paired t-test; n=7. Together, these results explain the dramatic effect of HCN blockade on L2/3 excitability (**Fig. 1**). The non-apparent sag potential at conventional hyperpolarizing current steps is thus surprising, suggesting a markedly faster occurrence of the I_h effect exists in L2/3 PCs which occludes the biphasic nature of the sag response. To investigate this possibility, we measured the time constant of the immediate voltage responses. We found a strong positive correlation between the amplitude of a passive current command and the voltage response time constant, which was abolished by Cs^+ bath application (**Fig. 2g**). This confirms that I_h has a strong effect during the initial phase of hyperpolarizing voltage responses, which may contribute to the lack of detectable sag potential at modest current injections. However, other biophysical mechanisms may also contribute to the muted sag effect in L2/3 PCs.

Next, we examined the voltage dependence and kinetic properties of I_h in L2/3 PCs in voltage clamp (**Fig. 2h**). Significant Cs^+-sensitive (1mM) currents were activated at subthreshold membrane potentials, with half-activation voltages more negative than the resting membrane

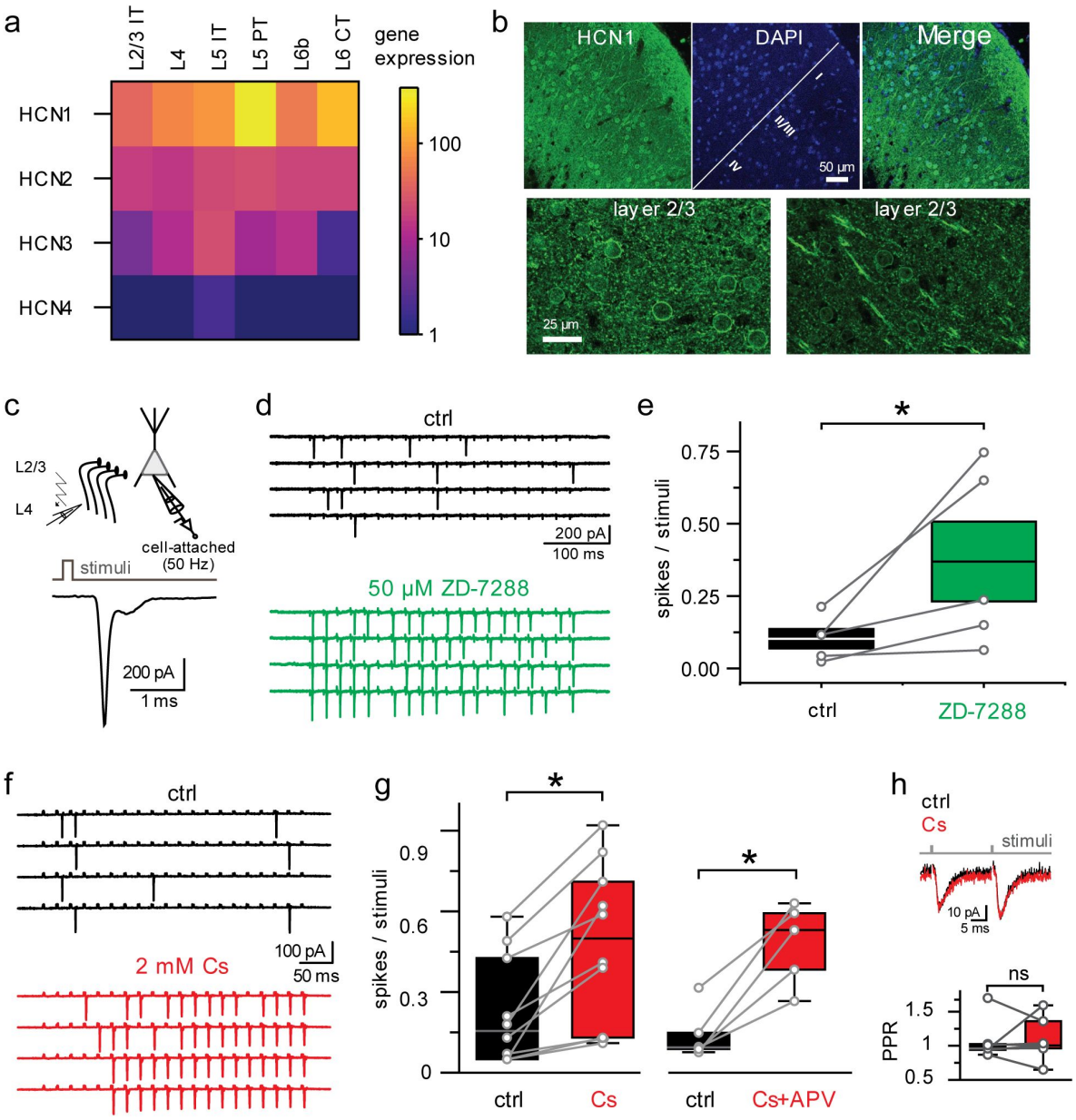

Fig 1.

HCN expression and effect of Cs^+ on AP firing in cortical L2/3 PCs

a. HCN gene subunits show uniform expression pattern among cortical PC types. Data is collected from the online available dataset(29). **b.** HCN1 immunohistochemistry reveals dense somatic expression in layer 2/3 of the visual cortex **c.** HCN channels control the excitability of L2/3 PCs. Schematic illustration of the experimental arrangement of cell attached recordings during extracellular stimulation of L4, and the shape of the elicited action potential. **d.** Representative traces showing increased firing upon ZD-7288 application. **e.** ZD-7288 increases the firing of L2/3 PCs upon electrical stimulation (0.1 ± 0.03 spikes/stimuli vs 0.4 ± 0.12 spikes/stimuli in control vs ZD-7288 application, respectively, p=0.04, t(4)=-3.0, Student's paired-sample t-test, n=5). **f.** Increased spiking of L2/3 PC upon blockade of HCN channels with 2 mM CsMeSO4 (right). **g.** Pharmacological block of I_h significantly increases the firing response of L2/3 PCs (0.22 ± 0.06 spikes/stimuli vs. 0.48 ± 0.09 spikes/stimuli for control vs CsMeSO4 bath application, p=0.002, t(9)=-4.42, Student's paired t-test, n=10. **h.** Presynaptic contributions were examined using the paired-pulse ratio (PPR) in whole cell current clamp recordings (1.09 ± 0.12 spikes/stimuli vs. 1.17 ± 0.15 spikes/stimuli for control vs CsMeSO4 bath application, p=0.422, t(6)=-0.8612, Student's paired t-test, n=7).

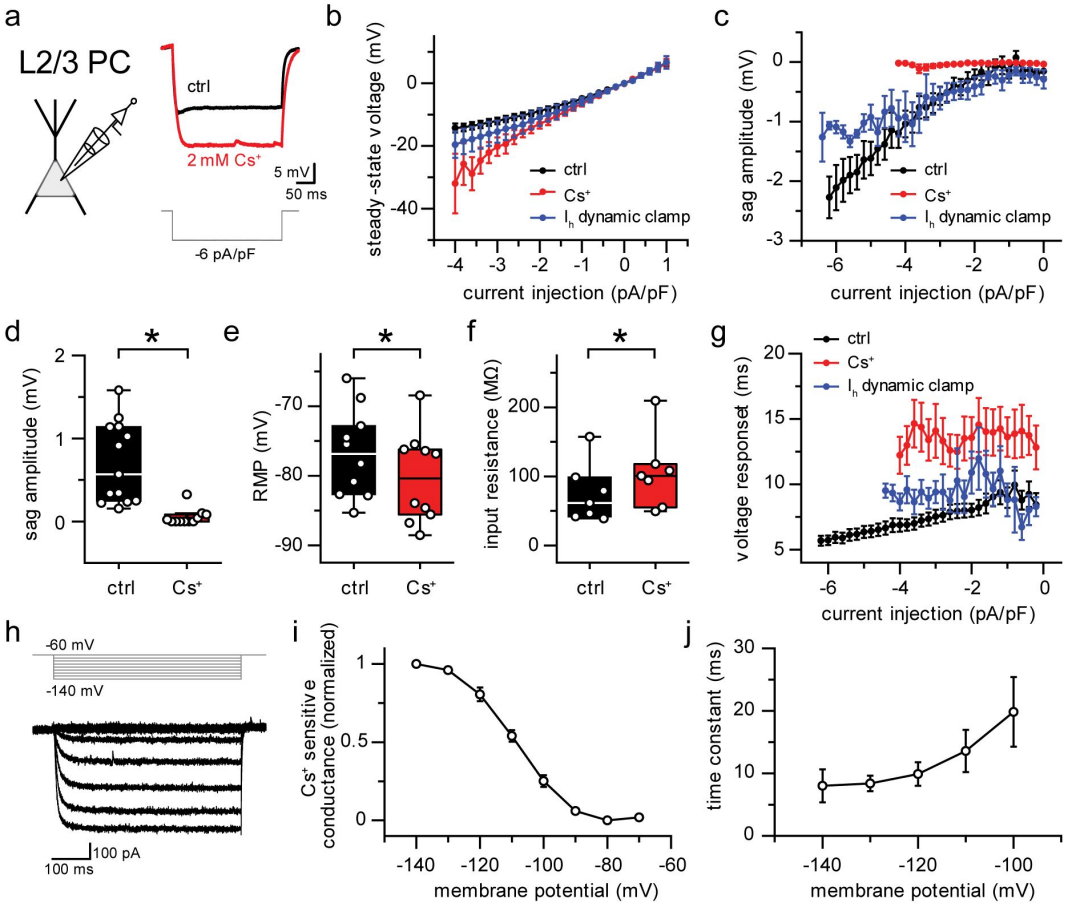

Fig 2.

Functionally relevant I_h in L2/3 PCs

a. Whole cell current clamp recordings showing the presence and absence of sag response to very negative current commands in control conditions (black) and upon Cs^+ application (red). **b.** Steady-state voltage response rectification upon hyperpolarizing current injections is mediated by I_h. **c.** Sag voltage is abolished by blocking I_h. **d.** Sag amplitude is Cs^+ sensitive (0.7 ± 0.49 mV vs. 0.05 ± 0.1 mV for control vs CsMeSO4 application, $p=2.46^{-4}$, t(22)=4.37, Student's two-sample t-test, n=13 and 11). **e.** Resting membrane potential is modulated by I_h (-76.75 ± 6.37 mV vs. -80.29 ± 6.48 mV for control vs CsMeSO4 bath application, $p=1.98^{-4}$, t(9)=6.02, Student's paired t-test, n=10). **f.** Input resistance is altered by I_h (74.78 ± 42.34 mV vs. 104.99 ± 52.91 mV for control vs CsMeSO4 bath application, p=0.048, t(6)=-2.48, Student's paired t-test, n=7). **g.** The time course of voltage responses to hyperpolarizing current on the magnitude of the current injection is abolished by Cs^+. **h.** Example voltage clamp recording of cesium sensitive currents in a L2/3 PC. **i.** Voltage dependence of cesium sensitive current activation, **j.** Voltage dependent activation kinetics of cesium sensitive currents.

potential, and with relatively fast activation kinetics (**Fig. 2i,j**). Overall the pharmacological profile, effects on passive electrical properties, and voltage dependence all point to previously published data describing HCN channels (31). Together these results indicate that L2/3 PCs express a functionally relevant population of HCN channels, which constrain the excitability of these cells. Similar responses were observed in voltage clamp recordings across several cortical regions (e.g., in S1, M1, and A1; **Supplementary Fig. 2**), suggesting that HCN channels are a consistent feature in L2/3 PCs.

Noncanonical subthreshold signal processing in L2/3 PCs by I_h

Electrical signals at different dendritic compartments undergo distance-dependent distortion (28, 32), which has a major effect on neuronal function in cells with extensive dendritic branching (33). To counteract these effects, larger L5 PT-type PCs and CA1 PCs express HCN channels with nonuniform distributions (19, 31). As L2/3 PCs have a much more compact morphology, synaptic input distortions might be less severe, raising the possibility of an alternative function of HCN channels in these cells. Thus, to investigate the distance-dependence of HCN on L2/3 synaptic inputs, we made whole-cell patch recordings from Alexa-594 filled L2/3 PCs and performed extracellular minimal stimulation at different dendritic locations guided with 2P microscopy (**Fig. 3a**). Elicited EPSPs likely reflect the activation of a single axon, as stimulus intensity was set to achieve an ~50% failure rate(34). As HCN deactivation has been shown to strongly impact the duration of synaptic events(28, 32), we quantified changes in the half-width of locally evoked EPSPs, here using the HCN-selective blocker ZD-7288 (50 μM). Surprisingly, our results were in contrast to previous reports in L5 PT-type and CA1 PCs, in that I_h block had a far smaller effect on the time-course of distally-evoked (>100 μm distance from the soma) synaptic responses. In contrast, proximal inputs (<100 μm) were markedly more broadened after I_h blockade (**Fig. 3b,c**). These results suggest that L2/3 PCs are equipped with a distinctive subcellular HCN distribution, potentially contributing to noncanonical distance-dependent input amplification along the dendritic axis of L2/3 cells.

Pathway-specific modulation of synaptic information

L2/3 PCs receive information from distinct brain regions, such as “top-down” (cortical-cortical) axons, generally arriving to layer 1(35) and “bottom-up” (thalamocortical/layer 4) axons, terminating on proximal dendrites located in layer 4 and 2/3 (36). Due to the stronger proximal effect of HCN on L2/3 PC EPSPs, we explored whether this modulation yielded input-pathway-specific differences. Whole- cell recordings were again obtained from L2/3 PCs, and EPSPs were elicited by minimal stimulation with electrodes situated to preferentially stimulate either layer 4 or layer 1 axons (electrode placement ~200μm laterally from recorded PC in either layer). Inhibition was left intact in these experiments. While most evoked EPSPs were small (< 0.5 mV), a subset evoked with minimal stimulation was outsized (we deemed these here as L4-Type I and L4-Type II inputs, respectively; **Fig. 3d**, **Supplementary Figure 3**). The L4-Type II events were substantially larger than previous reports(3) but see (37).

I_h blockade significantly broadened elicited EPSPs when the stimulation electrode was placed in layer 4, but not in layer 1 (**Fig. 3e**). Consequently, the effect of Cs^+ on the EPSP integral was significant for L4 inputs, but not L1 inputs (**Fig. 3f**). The effect of Cs^+ on EPSP half-width and voltage integral was similar for both L4-Type I and L4-Type II inputs, suggesting intermingled termination zones(36) in proximal dendrites. HCN channels are notable for their ability to restrain temporal integration of synaptic inputs(28). Therefore, we repeated these experiments using more high- frequency stimulation (5 stimuli at 50 Hz; **Fig. 3g**; inhibition was blocked due to strong inhibitory recruitment at 50Hz). In accordance with the effect on single EPSPs, summation of L1 (i.e., distal) inputs was unaltered with HCN block. In contrast, HCN blockade led

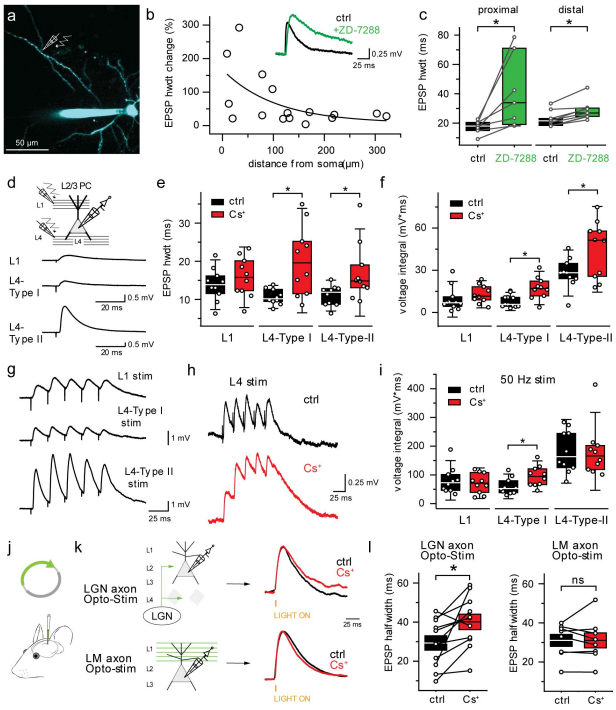

Fig 3.

Noncanonical effect of I_h block on EPSPs in L2/3 PCs

a. Experimental arrangement of extracellular targeted stimulation of a L2/3 PC dendrite. **b.** Application of ZD-7288 revealed a proximal bias for EPSP modulation by I_h (Exponential fit τ=104.7 µm, R^2=0.33, n=18). Inset shows a stimulating location 28 µm away from the soma in control conditions (black trace) and upon Z-7288 application (green trace). **c.** EPSP halfwidth is significantly modulated along the dendritic axis by I_h, (proximal dendritic locations: 17.42 ± 1.68 ms vs. 40.95 ± 24.78 ms for control vs 50µm ZD-7288 bath application, p=0.03, t(6)=2.84, Student's paired t-test, n=7, distal dendritic locations: 22.68 ± 1.78 ms vs. 28.65 ± 2.17 ms for control vs 50µm ZD-7288 bath application, p=2.1^{-4}, t(8)=-6.39, Student's paired t-test, n=9)**. d.** Schematic illustration of the experimental arrangement. L2/3 PCs were recorded in whole-cell current clamp mode, and a stimulating electrode was placed either in L1 or L4. **e.** I_h modulates EPSP halfwidth for L4 stimulation, but not for L1 (13.87 ± 1.37 ms vs. 15.8 ± 1.67 ms for control vs CsMeSO4 bath application in L1, p=0.38, t(18)=-0.89, Student's two- sample t-test, n=10 each, 10.65 ± 0.64 ms vs. 20.17 ± 2.88 ms for control vs CsMeSO4 bath application for L4-Type I inputs, p=0.005, t(18)=-3.22, Student's two-sample t-test, n=10 each, 11.01 ± 0.85 ms vs. 17.05 ± 2.41 ms for control vs CsMeSO4 bath application for L4-Type II, p=0.03, t(18)=-2.36, Student's two-sample t-test, n=10 each). **f.** Pathway-specific I_h effect on unitary EPSP voltage integral (9.35 ± 2.54 mV*ms vs. 12.9 ± 2.04 mV*ms for control vs CsMeSO4 bath application in L1, p=0.3, t(19)=-1.07, Student's two-sample t-test, n=11 and n=10 respectively, 7.85 ± 1.24 mV*ms vs. 17.39 ± 2.5 mV*ms for control vs CsMeSO4 bath application for L4-Type I inputs, p=0.002, t(20)=-3.6, Student's two-sample t-test, n=12 and n=10 respectively, 28.01 ± 3.45 mV*ms vs. 44.89 ± 6.42 mV*ms for control vs CsMeSO4 bath application for L4-Type II inputs, p=0.03, t(18)=-2.31, Student's two-sample t-test, n=10 each). **g.** Representative recordings of 50 Hz repeated extracellular stimuli (L1 – grey, L4-Type I – blue, putative L4-Type II -green). **h.** Temporal summation of L4-Type I input stimulation in control conditions (black) and during CsMeSO4 application (red). **i.** Pathway-specific I_h modulation of synaptic summation (81.05 ± 14.5 mV*ms vs. 71.07 ± 11.19 mV*ms for control vs CsMeSO4 bath application in L1, p=0.6, t(18)=0.54, Student's two-sample t-test, n=10 each, 60.06 ± 9.03 mV*ms vs. 95.15 ± 11.29 mV*ms for control vs CsMeSO4 bath application for L4-Type I, p=0.03, t(18)=-2.42, Student's two-sample t-test, n=10 each, 182.08 ± 23.36 mV*ms vs. 182.05 ± 28.59 mV*ms for control vs CsMeSO4 bath application for L4-Type II, p=0.99, t(18)=$8.74*10^{-4}$, Student's two-sample t-test, n=10 each). **j.** Schematic illustration of the experimental setup. Mice were injected with AAV.CAMKII.C1V1/eYFP either in the latermodial visual area (LM, to label axons arriving to L1) or in the LGN (to label proximal targeting axons). **k.** Example trace showing optogenetic activation of LM (top) and LGN (bottom) axons in control conditions (black) and upon Cs^+ application (red). Traces are normalized. Blue line marks the timing of the optogenetic stimulus. **l.** Cs^+ effect on optogenetically elicited EPSPs from cortico-cortical (LM, left; 35.06 ± 3.06 vs. 31.04 ± 3.82 for control vs Cs^+ respectively, p=0.99, t(7)=0.001, Student's paired-sample t-test, n=8) and thalamic (LGN, right; 29.31 ± 3.68 vs. 40.11 ± 3.95 for control vs Cs^+ respectively, p=0.01, t(10)=- 2.95, Student's paired-sample t-test, n=11) sources.

to increased temporal summation of L4-Type I inputs (**Fig. 3h,i**). Summation of L4-Type II inputs was not affected by HCN channel block, suggesting further diversification between L4-Type I and L4-Type II inputs as well.

To more accurately evaluate whether synaptic signaling from *bone fide* bottom-up and top- down axons are differentially regulated by HCN, we next injected a CaMKII-driven, C1V1-expressing AAV into either the LGN or the lateromedial visual (LM) areas in separate experiments (LM, **Fig. 3j,k**). LGN and LM-originating axons are thought to preferentially synapse onto proximal and distal L2/3 dendrites, respectively (38–41). In these experiments, short LED-directed amber light pulses could reliably elicit EPSPs in L2/3 PCs (**Fig. 3k**). We used a 'minimal' opto stim approach for these experiments, meaning we used as low light power as possible to reliability (1 ms pulses at 0.2 Hz) evoke EPSPs, while avoiding AP firing and thus further network recruitment. Inhibition was not blocked during optical stimulation. These optogenetic experiments revealed a negligible effect of Cs^{+} on top-down, LM-driven EPSPs. Conversely EPSPs were significantly broadened following Cs^{2+} of bottom-up, LGN-originating EPSPs (**Fig. 3k,l**). Together these results suggest that HCN channels preferentially regulate thalamic-originating, bottom-up nonlinear signaling in proximal dendritic regions of L2/3 PCs.

I_h channels constrain NMDA receptor-dependent synaptic boosting in proximal dendrites

In a passive environment, dendritic filtering(42) creates attenuated (i.e., wider) EPSPs when originating further from the soma. Yet our results show an opposite phenomenon with HCN channels blocked. It has been described that reduced HCN availability can facilitate dendritic boosting mechanisms via activation of either voltage-gated(43) or NMDA(44) channels. To investigate possible contributions of dendritic voltage-dependent processes, we next performed NEURON computational simulations using a realistic L2/3 PC dendritic morphology(45). Inserting voltage-gated sodium or potassium channels with various distributions could not recapitulate our distance-dependent EPSP observations (**Supplementary Figure 4**.). Thus, we next investigated whether NMDA receptors might play a role in the observed phenomenon due to their described overwhelming contribution to *in vivo* activity in L2/3 PCs (8, 46).

We first tested whether NMDA receptors contribute to spontaneously occurring synaptic inputs (sEPSPs) in L2/3 PCs(47) in slice experiments. Due to potential alterations in spontaneous release and overall circuit activity, extracellularly applied NMDA blockers may introduce significant confounds for this line of investigation especially as spontaneous synaptic potentials show tremendous variability in frequency, amplitude, and kinetics. To overcome this conundrum, we designed a custom-built pipette attachment through which the intracellular solution could be stably exchanged during whole- cell recordings (48). We recorded sEPSPs in L2/3 PCs first using control intracellular solution, which was then exchanged to a 50 µM MK-801 (non-competitive NMDA receptor antagonist) containing intracellular solution (**Fig. 4a**). To also capitalize on the voltage-sensitivity of NMDA receptors, average peak amplitudes were recorded at two different membrane potentials for each intracellular condition; -80 mV and -55 mV (resting membrane potential, and a somatic membrane potential depolarized enough to partially unblock NMDA receptors (49)). Due to the small nature of L2/3 PC sEPSPs, quantification of other waveform parameters (i.e., EPSP width) was avoided. After quantifying the mean sEPSP peak at -80 mV, we calculated the expected (linear) sEPSP peak at -55 mV and compared this prediction to our observations of -55 mV. We found that sEPSPs were significantly larger than predicted after depolarization (**Fig. 4b**), alluding to the presence of a nonlinear subthreshold amplifying mechanism. We found that intracellular MK-801 solution exchange could severely dampen this synaptic amplification (**Fig. 4c**), indicating that NMDA receptors actively contribute to shaping naturally occurring sEPSPs in L2/3 PCs. The effect of pipette perfusion itself on our measurements was negligible (**Supplementary Fig. 5**)

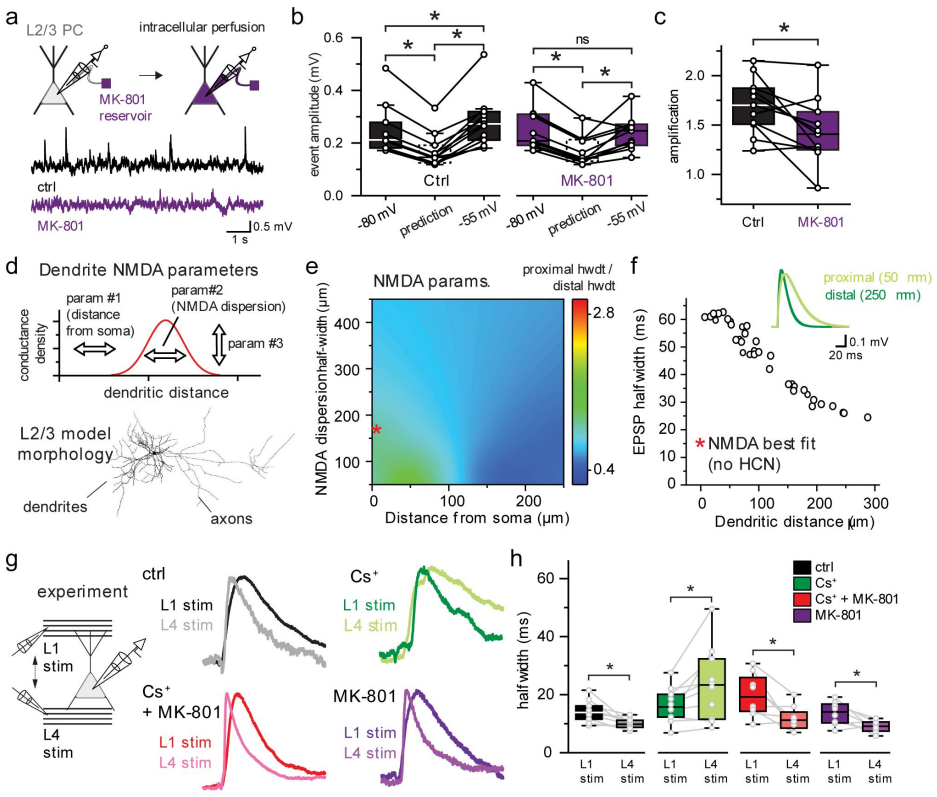

Fig 4.

Pathway-specific NMDA receptor boosting of synaptic information

a. Schematic illustration of intracellular pipette solution perfusion during whole-cell patch clamp recordings. Briefly, the pipette was filled with control recording solution (black trace), which was exchanged to an intracellular solution containing 50 µM MK-801 (purple trace) during the recording. **b.** Mean peak amplitude of sEPSPs measured at two different membrane potentials and two different recording conditions (ctrl -80 mV vs. ctrl prediction: $p=4.72*10^{-6}$, t(10) = 8.86, ctrl -80 mV vs ctrl -55 mV: p=0.02, t(10) = -2.81, ctrl prediction vs ctrl -55 mV: $p=1.63*10^{-5}$, t(10) = -7.71, MK-801 -80 mV vs. MK-801 prediction: $p=1.15*10^{-6}$, t(10) = 10.36, MK-801 -80 mV vs MK-801 -55 mV: p=0.58, t(10) = 0.57, MK-801 prediction vs MK-801 -55 mV: $p=2.69*10^{-3}$, t(10) = -3.95, Student's paired-sample t-test, n = 11 for each). **c.** Synaptic amplification estimated by dividing the predicted peak amplitude from the hyperpolarized recordings and the measured peak at depolarized membrane potentials (1.69 ± 0.09 and 1.43 ± 0.1 for ctrl and MK-801 amplification respectively, p=0.01, t(10) = 3.04, Student's paired-sample t-test, n=11). **d.** Schematic illustration of the multiparameter NEURON fitting procedure for dendritic NMDA. Conductance localization, dispersions, and conductance densities of NMDA were varied along a somato-dendritic axis as set by a Gaussian curve, which was shifted in space, in peak, and in width (top panel). Simulations were carried out using fully reconstructed L2/3 PC from the Allen Institute open-source database (bottom panel). **e.** Inserting NMDA receptors into proximally located simulated synapses recreated the experimentally determined distance-halfwidth relationship. Notice the best fit of the control conditions (where proximal/distal EPSP halfwidth is similar), is characterized by a Gaussian curve with proximal peak center with a moderate width (dispersion). **f.** Best fit of the distance-dependent EPSP halfwidth with no HCN in the system. Red asterisk denotes the best fit parameter-space on panel. Proximally (gray) and distally (black) originating EPSPs from the model are shown in the inset. **e. g.** Amplitude-normalized EPSPs recorded from L2/3 PCs by minimal stimulation in either in L1 (dark color tones) or L4 (light color tones) in different recording conditions (ctrl: *black*, extracellular cesium: *green*, extracellular cesium + intracellular MK-801: *red*, intracellular MK-801: *purple*). Cells were recorded for each pharmacological condition independently with L4 and L1 stimulation occurring in each recording. **h.** As predicted (panel f) proximal inputs from L4-originating EPSPs were faster than those from distal L1 synapses in control conditions. The broadening effect of cesium on L4 (proximal) originating EPSPs is occluded by NMDA receptor block (14.25 ± 1.17 ms and 10.11 ± 0.56 ms for L1 vs L4 stimuli in control conditions, $p=6.73*10^{-3}$, t(9)=3.5, Student's paired-sample t-test, n=10 each, 16.22 ± 1.91 ms and 23.61 ± 4.04 ms for L1 vs L4 stimuli during Cs bath application, p=0.03, t(9)=-2.67, Student's paired-sample t-test, n=10 each, 19.92 ± 2.65 ms and 11.8 ± 1.55 ms for L1 vs L4 stimuli during Cs bath application and MK-801 intracellular application, p=0.02, t(7)=3.01, Student's paired-sample t-test, n=8 each, 13.62 ± 1.43 ms and 8.97 ± 0.72 ms for L1 vs L4 stimuli during MK-801 intracellular application, p=0.025, t(7)=2.84, Student's paired-sample t-test, n=8 each).

Having established that NMDA receptors play an active role in modulating sEPSPs, we next utilized computational simulations to explore whether non-uniform NMDA recruitment could explain the subthreshold boosting in proximal L2/3 synapses, as described earlier following HCN channel blockade (**Fig. 3b**). Accordingly, this initial model did not include HCN channels. NMDA was inserted into a NEURON model with varying distributions and conductance densities (**Fig 4d**) to systematically evaluate a large parameter space. These simulations (**Fig. 4e**) revealed that a proximally-biased NMDA distribution (50) could indeed produce local EPSP boosting (**Fig. 4e,f**) similar to our experimental findings in an HCN-lacking condition.

Because HCN channels can reduce NMDA recruitment during synaptic signaling, we next explored whether proximal enrichment of HCN allows for bottom-up-specific gating of NMDA amplification (**Fig. 4e,f**) now using complimentary slice experiments. To accomplish this, we recorded L2/3 EPSPs originating from both proximal L4 and distal L1 inputs during each recording (i.e., two stimulation locations for each cell; **Fig. 4g**). For each recording, one pharmacological condition was evaluated to sequentially explore the interplay between HCN and NMDA (**Fig. 4g**). In control conditions, L4-evoked EPSPs were slightly narrower than L1-evoked EPSPs. This layer-specific relationship was inverted following extracellular Cs^+ to block HCN (**Fig. 4g,h**). This result recapitulated our NEURON simulation best-fit prediction, where a proximally-biased NMDA distribution was necessary (**Fig. 4f**).

To confirm that this L4-specific EPSP broadening after HCN channel block was indeed due to NMDA-inducted boosting, as predicted in our simulations (**Fig. 4f**), we next examined L4 and L1- evoked EPSPs using Cs^+ and intracellular MK-801. In the presence of internal MK-801, the broadening effect of Cs^+ on L4-evoked EPSPs was abolished, thereby reverting the L4-L1 EPSP relationship to a control-like state. (**Fig. 4g,h**). The NMDA receptor contribution is unlikely related to different event amplitudes in proximal and distal sources, as the peak and halfwidth of the elicited EPSPs in our dataset showed no correlation (**Supplementary Fig. 6**). Together, our modeling and experimental results indicate that NMDA-directed amplification of L4 inputs is strongly constrained by a proximal HCN bias in L2/3 PCs dendrites, allowing for pathway-specific modulation of 'bottom-up' inputs without affecting those arriving from 'top-down' L1 axons.

Noncanonical HCN distribution predicted in L2/3 PCs

We next carried out a more complete computational simulation which included both HCN and NMDA in a L2/3 PC. To test whether our results could be explained due to a non-uniform HCN distribution, HCN channels were inserted into the model with varying distributions and conductance densities (**Fig 5a**) to evaluate a large parameter space. Our simulations revealed that proximal bias in HCN channel distributions could best recapitulate our observations of proximally and distally originating EPSP waveforms in control conditions (**Fig. 5b,c**). This is in line with the proximal HCN1 channel staining (**Fig. 1**) revealed by immunohistochemistry. Together our results indicate that L2/3 PCs have a proximal HCN channel bias, whereas previous studies found a distal dendritic HCN bias in L5 PT-type PCs and CA1 PCs(19, 31), which could constrain NMDA receptor amplification in an input-specific manner.

Tight developmental upregulation of Layer 2/3 HCN channels

Due to the ability of HCN channels to regulate NMDA boosting shown earlier, modifying HCN availability or expression may represent an important activity or plasticity gate in L2/3. Previously we found that HCN recruitment was upregulated in interneurons during early development(51). Indeed, several ion channels show postnatal maturation in their biophysical properties and surface expression(52), raising the possibility of a different proximo-distal HCN bias in young L2/3 PCs compared to adult animals. To examine this possibility, L2/3 PCs were recorded at three developmental time points (1^{st}, 2^{nd} and 6^{th} postnatal week) in S1 cortex. Our assessment showed that a rapid developmental HCN upregulation occurs between 1 and 2 weeks

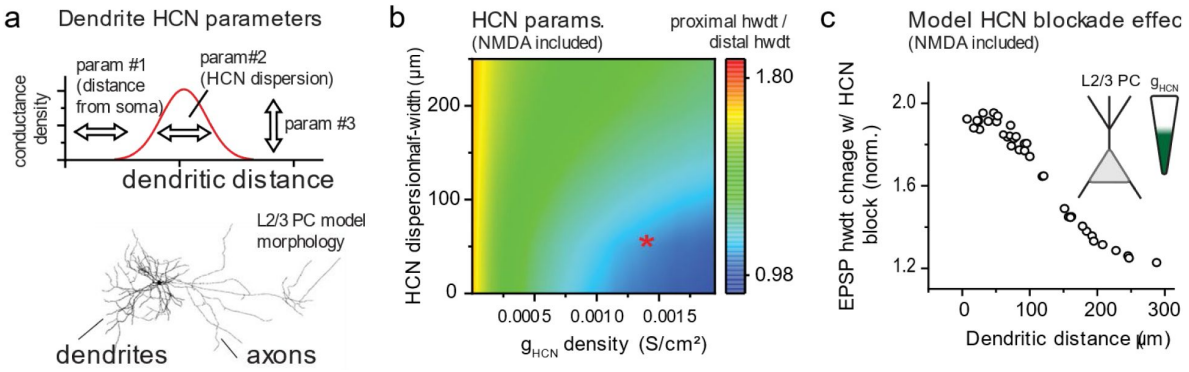

Fig 5.

Proximal bias in HCN channel expression dampens proximal NMDA receptor-dependent synaptic boosting in a NEURON model simulation.

a. Schematic illustration of the multiparameter NEURON fitting procedure for dendritic HCN. Simulations here included the NMDA dendritic parameters established in **Fig. 4**. HCN conductance localization, dispersions, and conductance densities were varied along the somato-dendritic axis as set by a Gaussian curve, which was shifted in space, in peak, and in width as well (top panel). Simulations were carried out using fully reconstructed L2/3 PC from the Allen Institute open-source database (bottom panel). **b**. A proximal abundance bias of HCN channels recapitulates experimental findings in control conditions. Best fit in the parameter space tested is denoted with red asterisk, where a high density of HCN channels were proximally localized. **c.** Model-derived data showing the effect of HCN blockade in the best-fit scheme when NMDA is also included as shown in **Fig. 4**. Note that the effect of HCN removal in this model closely recapitulates our experimental findings using ZD-7288 earlier.

old. We also found that 1 week old L2/3 PCs displayed markedly different passive properties, while 2-week-old cells were quite similar to mature cells (**Fig. 6a**). The non-quantifiable sag potential in 1 week old animals implies the lack of I_h current at this developmental time point, however, the disproportionately large input resistance and elevated resting membrane potential also suggests that other background leak channels may also be missing at this developmental window (**Fig. 6b**). Subsequent voltage clamp recordings confirmed that in 1 week old animals, L2/3 PCs do not possess a considerable amount of I_h in contrast to 2 and 6 week old animals (**Fig. 6c,d**). We found that both the resting membrane potential and peak I_h conductance changes throughout development were tightly (negatively) correlated (**Fig. 6e**). This provides additional evidence for parallel maturation of HCN with other leaky channels, as HCN channel expression alone would be predicted to shift the membrane to more depolarized potentials (**Fig. 2e**).

Next, we mapped the distance-dependence dendritic EPSP kinetics in 1 week old animals (**Fig. 6f**). We found a surprising 'non-Rallian' negative correlation between EPSP halfwidth and stimulation distance from the soma (**Fig. 6g, h**), similar to our previous results from mature neurons with HCN channels blocked (**Fig. 3a,b**). This suggests the presence of nonlinear boosting mechanisms (e.g., NMDA) in proximal dendrites of developing L2/3 PCs, similar to mature cells, but which are unabated due to the lack of HCN at this early developmental stage.

I_h dependent neuromodulation of L2/3 PC activity by serotonergic inputs

Whether the mature brain possesses mechanisms to modulate HCN in L2/3 PCs is unknown. Nonetheless, previous work in cortical L5 PT-type PCs shows that I_h currents can be modulated following 5-HT_7 serotonergic receptor activation(53). L2/3 PCs are extensively innervated by serotonergic axons from the dorsal raphe (54), providing a potential framework to modify HCN availability. Single-cell RNA-seq (29) showed that L2/3 PCs do express 5-HT_7 receptors, interestingly, at higher levels than all other cortical PCs (**Fig. 7a**). We pharmacologically evaluated a potential role of serotonergic HCN regulation by bath application of 5-carboxamidotryptamine (5-CT; 30 nM), a specific 5-HT_7 agonist. 5-CT application significantly reduced evoked firing of L2/3 PCs during extracellular stimulation in L4 (**Fig. 7b**). Current clamp experiments revealed that the rectification of steady-state voltage responses to hyperpolarizing current injection was amplified with 5-CT (**Fig. 7c**), likely due to the increased availability of HCN channels due to a rightward shift in their activation voltage-dependence (**Fig. 7d**). 5-CT also reduced L2/3 input resistance potentially via HCN regulation, however, did not yield a depolarizing effect on the resting membrane potential nor affect AP threshold (**Fig. 7e**). Importantly, 5-CT had no impact on the firing responses of L2/3 PCs when I_h currents were blocked with background Cs^+ throughout the experiment (**Fig. 7f**). Furthermore, the dampening of neuronal output was not related to an downregulating effect of 5-HT7 on NMDA receptors (**Fig. 7g**, (55)). Together these results indicate that neuromodulation represents an endogenous mechanism by which HCN availability can be altered in L2/3 PCs. Further studies on the input-specific effects of neuromodulation on dendritic nonlinearities in L2/3 PCs should thus be considered.

Discussion

Precise communication between cortical neurons relies on discrete pre- and postsynaptic forms of information transfer at synapses. The majority of cortical synapses terminate along the dendritic tree (56) where, based on local active and passive electrical properties, various types of nonlinear transformations occur. The spatially and electrically disjointed nature of dendrites (57) from the rest of the cell allows for local, soma-independent computation. For example, perturbing active dendritic elements (i.e., local conductances) can impair several fundamental

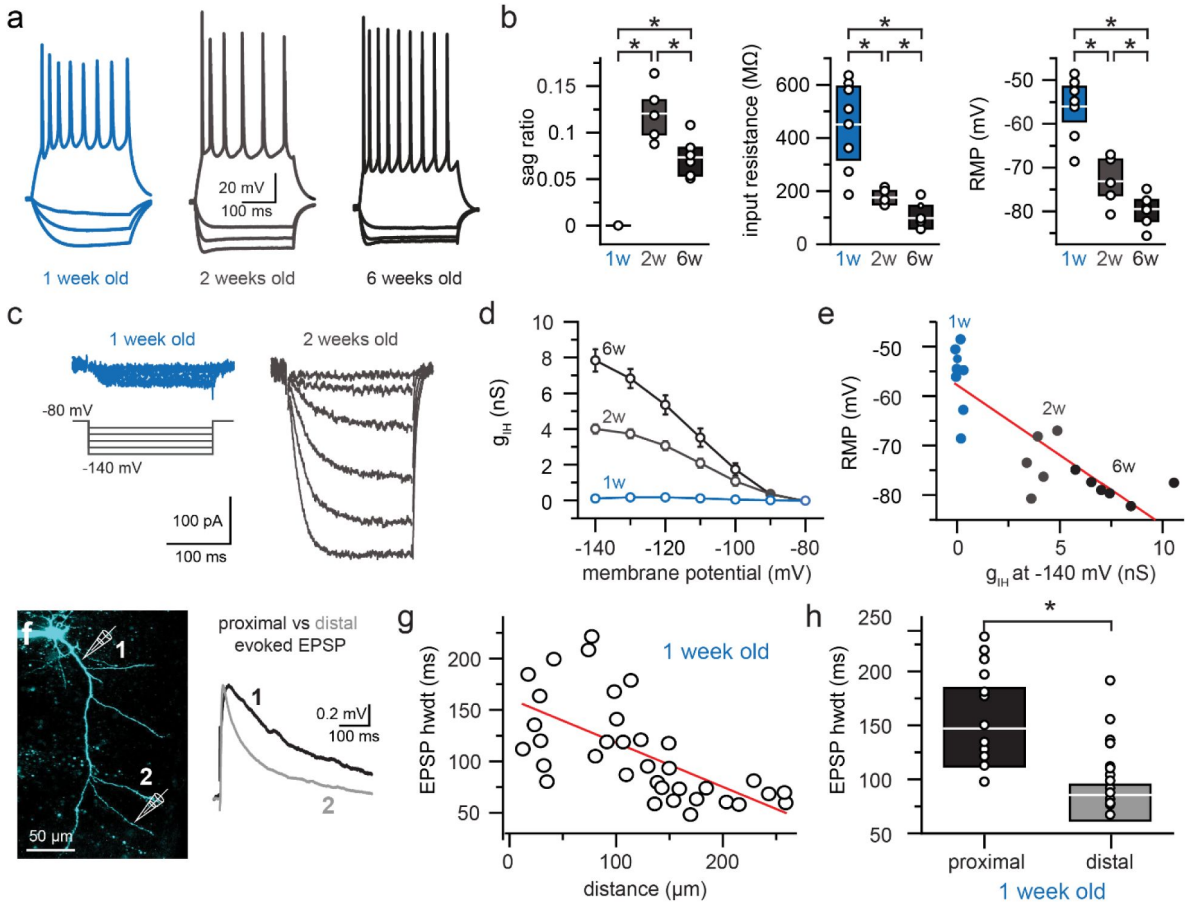

Fig 6.

Developmental regulation of I_h expression

a. Representative firing patterns recorded from one week old (left, blue), two weeks old (middle, grey) and six weeks old L2/3 PCs. **b.** Developmental regulation of sag ratio (0.0 ± 0.0, 0.12 ± 0.01 and 0.07 ± 0.01 for one- (n=8), two- (n=5) and six week old L2/3 PCs (n=6), respectively, p=0 for one week old vs two weeks old cells, p=0.01, t(9)=3.04 for two vs six weeks old cells and p=0 for one vs six weeks old cells, Student's two-sample t-test), input resistance (450.6 ± 57.91 MΩ, 175.66 ± 13.66 MΩ and 98.34 ± 18.86 MΩ for one- (n=8), two- (n=5) and six week old L2/3 PCs (n=7), respectively, p=0.004, t(11)=3.65 for one week old vs two weeks old cells, p=0.01, t(10)=3.06 for two vs six weeks old cells and $p=1.11*10^{-4}$, t(13)=5.54 for one vs six weeks old cells, Student's two-sample t-test) and resting membrane potential (-56.05 ± 2.33 mV, -73.13 ± 2.55 mV and -79.47 ± 1.33 MΩ for one- (n=8), two- (n=5) and six week old L2/3 PCs (n=7), respectively, $p=5.9*10^{-4}$, t(11)=4.76 for one week old vs two weeks old cells, p=0.04, t(10)=2.39 for two vs six weeks old cells and $p=1.36*10^{-6}$, t(13)=8.37 for one vs six weeks old cells, Student's two-sample t-test). **c.** Representative voltage clamp recordings of hyperpolarization activated currents in one week old (left, blue), two weeks old (middle, gray) and six weeks old L2/3 PCs (right, black). **d.** Voltage dependence of hyperpolarization activated currents in one week old (blue), two weeks old (gray) and six weeks old L2/3 PCs (black). **e.** Negative correlation between measured hyperpolarization activated current and resting membrane potential during development (Linear fit (red) slope: -2.84 mV/nS, intercept: -57.67 mV, R^2=0.71, n=20). **f.** Two- photon microscopy image depicting a proximal and a distal extracellular stimulating location positioned closely to an Alexa-594 filled L2/3 PC dendrite (left), and the resulting EPSPs (proximal – black, distal – green). **g.** EPSP halfwidth decreases with dendritic distance (Linear fit (red) slope: -0.42 ms/µm, intercept: 161.01 ms, R^2=0.4, n=35). **h.** EPSPs were significantly slower in proximal dendritic locations (147.07 ± 12.87 ms and 85.57 ± 6.83 ms for proximal and distal events, respectively, $p=5.31*10^{-5}$, t(33)=4.64, Student's two-sample t-test, n=13 and 22, respectively).

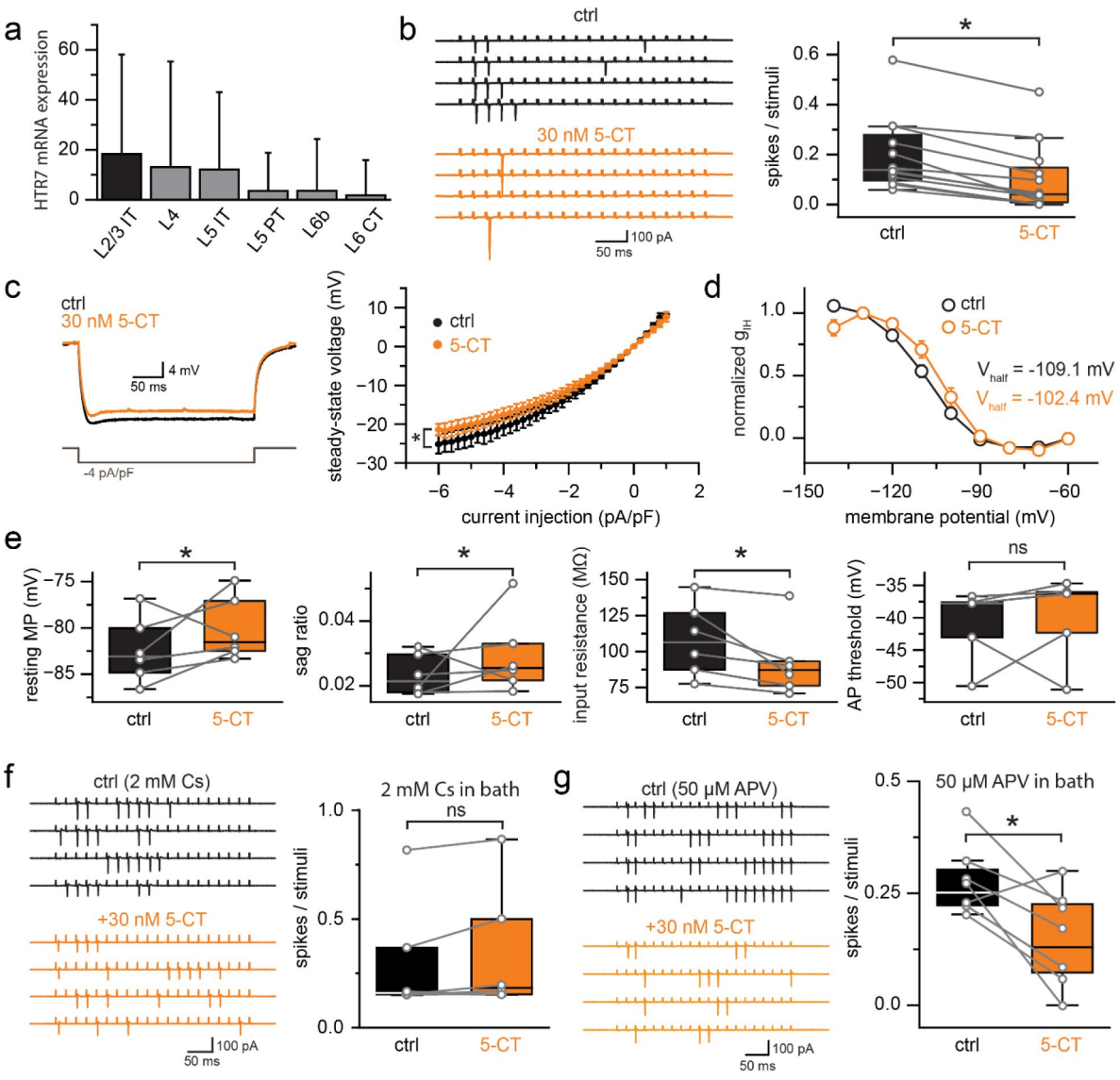

Fig 7.

Neuromodulation shifts L2/3 PC excitability via HCN channels

a. $5HT_7$ receptor mRNA is abundantly expressed in L2/3 PCs. Data is collected from the online available dataset(29). **b.** Example cell attached recording of a L2/3 PC (left) upon 50 Hz extracellular stimulation in L4 in control conditions (black) and 5-CT bath application (orange). 5-CT significantly reduced L2/3 PC spiking (0.2 ± 0.04 spike/stimuli vs. 0.1 ± 0.04 spike/stimuli for control vs 5-CT application, $p=3.57*10^{-6}$, t(11)=7.92, Student's paired-sample t-test, n=12 each) **c.** Example current clamp recording of voltage responses to hyperpolarizing current injections (left; control – black, 5-CT – orange). Steady-state voltage response rectification is amplified by $5HT_7R$ blockade (right). **d.** 5-CT shifts the voltage dependence of hyperpolarization activated currents (-109.06 ± 0.47 mV vs -102.35 ± 1.09 mV half activation for control vs 5-CT bath application, R^2 = 0.99 for both). **e.** 5-CT did not alter resting membrane potential (-82.41 ± 1.43 mV vs -80.14 ± 1.38 mV in control vs 5-CT bath application, respectively, p=0.89, t(5)=-1.41, Student's paired-sample t-test, n=6 each), sag ratio at -2 pA/pF current injection ($0.02 \pm 2.55*10^{-3}$ vs 0.03 ± 0.01 in control vs 5-CT bath application, respectively, p=0.82, t(5)=-1.01, Student's paired-sample t-test, n=6 each) and action potential threshold (-41.13 ± 2.6 mV, -40.08 ± 3.05 mV in control vs 5-CT bath application, respectively, p=0.64, t(4)=-0.4, Student's paired-sample t-test, n=5 each), but significantly reduced input resistance (108.21± 10.3 mΩ, 92.29 ± 9.9 MΩ in control vs 5-CT bath application, respectively, p=0.02, t(5)=2.75, Student's paired-sample t-test, n=6 each). **f.** Example recording showing no effect of 5-CT bath application when HCN channels were blocked (left: example recordings, right: 0.3 ± 0.11 spike/stimuli vs 0.34 ± 0.12 spike/stimuli in control vs 5-CT bath application, respectively, p=0.13, t(5)=-1.81, Student's paired-sample t-test, n=6 each). **g.** NMDA independent 5-CT effect on L2/3 PC excitability (0.27 ± 0.03 spike/stimuli vs 0.14 ± 0.04 spike/stimuli in control vs 5-CT bath application, respectively, p=0.01, t(7)=3.66, Student's paired-sample t-test, n=7 each).

cortical circuit tasks (36) such as perception (14), underlining the necessity for compartmentalized information processing. Further, single-subunit model simulations are unable to reproduce *in vivo* observed activity patterns of L2/3 PCs(9). Here, by combining *ex vivo* current clamp, synaptic stimulation, and ion channel recordings with empirically informed, biophysically realistic simulations, we demonstrate that L2/3 PCs in sensory cortex express a previously unappreciated, proximally-biased HCN channel distribution. Due to an apparent universal HCN expression in L2/3 cells from each cortical region, this arrangement should allow for modification of synaptic gain across all primary sensory areas of cortex. One of the basic functions of L2/3 PCs in sensory cortex is to encode first-order information, such as the orientation of visual input(2, 58, 59). Several investigations propose that arithmetic summation of a number of similarly tuned synapses will dictate whether these neurons will fire in response to sensory input (60). However, numerous dendritic nonlinearities have been established in L2/3 PCs, such as NMDA receptors (8), sodium channels (11), and calcium channels (10, 61), which also contribute to this process. Here we demonstrate that L2/3 PCs express a functionally relevant population of HCN channels well situated to modify the gain of cortical sensory and contextual information processing.

We report that HCN channels in L2/3 constrain fundamental aspects of cellular excitability, such as input resistance and resting membrane potential. This is likely due to a strong proximal somato-dendritic distribution of HCN channels, as observed in immunohistochemical experiments here. Likely due to their influence on input resistance, HCN blockade resulted in greatly increased AP firing during extracellular stimulation. L2/3 HCN channels strongly dampened excitatory synaptic inputs, however, only to those arriving at proximal dendritic locations. In line with this result, HCN channels reduced the timecourse of synaptic inputs following local stimulation in L4, but left those following L1 stimulation unaffected. Together with additional input-specific pharmacological experiments, NEURON simulations demonstrated that this input-specific synaptic phenomenon could indeed be explained by a proximal HCN channel distribution in dendrites putatively situated in L4 and L2/3. This was apparently only possible with a concurrent proximal NMDA recruitment bias. This predicted global organization should not be confused with observed differences in NMDA recruitment along the axis of individual L2/3 basal dendrites (47). Our predictions of NMDA distributions require further evaluation at the spine-synapse level. Although a proximal-basal dendrite NMDA receptor distribution is in line with findings from L5 PT-type PCs (62), HCN channels are instead enriched distal dendritic compartments in these PC types (19, 31). Thus the unique proximal HCN recruitment in L2/3 PCs permits pathway-specific control of synaptic amplification, as bottom-up (i.e., L4 originating) inputs target proximal dendritic compartments homogeneously (36). This was in opposition to top-down inputs, whose axons largely target distal dendrites in L2/3 PCs (63), as these synapses were unaffected by HCN channel blockade. To fully understand how compartment-specific pathways are functionally regulated, further anatomical and *in vivo* imaging experiments are needed to establish the distribution and synaptic dynamics of L4 and L1 inputs along the L2/3 PC dendritic tree.

HCN channels appear well suited to regulate the synaptic and intrinsic properties of L2/3 PCs, for example, if their availability is plastic or developmentally regulated. Previously, we found that HCN channel availability was upregulated in GABAergic interneurons during development, resulting in reduced propagation of subthreshold signals in mature axons (51). Interestingly, we found that L2/3 PCs in young animals (1 week old) lacked HCN currents. Together, these results suggest a universal developmental HCN upregulation across neuron types. In L2/3 PCs, the HCN channel maturation window was rapid and almost complete by the second postnatal week. Therefore critical period plasticity (64) and developmental I_h upregulation occur during a similar developmental window, suggesting a causal relationship. In addition to the robust developmental regulation of HCN channels, we also found that modification of HCN channel availability was also possible in the adult cortex, following serotonergic (5-HT_7) receptor-mediated biophysical regulation. This was likely due to a metabotropic process that increases cytosolic cAMP levels by stimulating adenylate cyclase(65) which in turn modulates HCN channel properties.

This raises the intriguing possibility that neuromodulation could induce nonstationary conditions in mature L2/3 circuits, for example, in re-biasing of bottom-up vs. top-down information, experience-dependent plasticity (66), or even for reopening of critical window-like states (67). A recent finding demonstrated increased spine density and stability during early development due to enhanced 5-HT release in L2/3 PCs of the prefrontal cortex(68), which suggests that serotonin is responsible for not only the morphological, but the physiological regulation of L2/3 PC spines as well.

As L2/3 PCs are one of the most abundant cell populations of the neocortex, HCN channels in these cells may exert overwhelming control over cortical excitability and thus cognition and memory. Cell non-autonomous HCN channel dysregulation manifests in clear behavioral changes, such as altered spatial learning (69) or impaired working memory (70). Curiously, higher HCN1 protein levels in the postmortem brain also correlate with cognitive resilience in aging humans (71). Therapeutic HCN channel modulation aimed at restoring healthy brain function in distinct pathophysiological states has consequently garnered significant interest (72–74), as both HCN1 and HCN2 are linked to neuropathic pain (75) and for treating major depressive disorder (73, 74, 76). Here we demonstrate that activation of the serotonergic receptor 5-HT_7 alters HCN channel function in L2/3 PCs, resulting in reduced PC excitability, similar to L5 PT-type PCs (53). 5-HT_7 receptor targeting agents are highly effective psychopharmacological compounds. Agents such as the antidepressant *vortioxetine* has a relevant therapeutic concentration that functionally suppresses 5-HT_7 (77), and the mood-stabilizing antipsychotic agent *lurasidone* possesses an even higher binding affinity to 5-HT_7 (78). Commonly used anesthetic drugs also modulate HCN channel action (79, 80), implying the need to investigate anesthesia-related mechanisms and confounds in L2/3 in both therapeutic and experimental settings. Together, we argue that HCN channels are present and functionally relevant in L2/3 PCs. As L2/3 PCs are one of the largest cell populations in the brain, and as HCN channels are the target of several current therapeutics, future research should consider their role in these cells in basic and clinical studies.

Methods

Acute slice preparation

All animal procedures were approved by the Emory University IACUC. Acute slices from cortex were prepared from mature C57Bl/6J mice (6–10 weeks old). Male and female mice were used for all experiments with data collected from ≥3 mice per experimental condition. Mice were first anesthetized with isoflurane and perfused with ice-cold cutting solution (in mM) 87 NaCl, 25 $NaHO_3$, 2.5 KCl, 1.25 NaH_2PO_4, 2 $MgCl_2$, 1 $CaCl_2$, 10 glucose, and 75 sucrose. Thereafter, mice were terminated by decapitation and the brain immediately removed by dissection. Brain slices (250 µm) were sectioned in the coronal plane using a vibrating blade microtome (VT1200S, Leica Biosystems) in the same solution. Slices were collected from V1 and from S1, M1 and A1 for a subset of experiments. Slices were transferred to an incubation chamber and maintained at 34°C for ~30 min and then at 23–24°C thereafter. During whole-cell recordings, slices were continuously perfused with (in mM) 128 NaCl, 26.2 $NaHCO_3$, 2.5 KCl, 1 NaH_2PO_4, 1.5 $CaCl_2$, 1.5$MgCl_2$, and 11 glucose, maintained at 30.0°C ± 0.5°C. All solutions were equilibrated and maintained with carbogen gas (95% O_2/5% CO_2) throughout.

Intracranial viral injections

5-8 week old mice were injected with AAV.CAMKII.C1V1/eYFP (0.2 µl total) in the lateromedial visual area (LM) or the lateral geniculate nucleus (LGN). During intracranial injections mice were head-fixed in a stereotactic platform (David Kopf Instruments) using ear bars, while under isoflurane anesthesia (1.5-2.0%). Thermoregulation was provided by a heating plate using a rectal thermocouple for biofeedback, thus maintaining core body temperature near 37°C. Bupivacaine was subcutaneously injected into the scalp to induce local anesthesia. A small incision was opened

5-10 minutes thereafter and a craniotomy was cut in the skull (< 0.5 µm in diameter) to allow access for the glass microinjection pipette. Coordinates (in mm from Bregma) for microinjection in the LM were X = ± 3.5; Y = -3.87; α = 45°; Z = 0.7, coordinates for the LGN were X = ± 2.0, Y = -2.0; α = 0°; Z = -2.45. Viral solution (titer 1 x 10^{13} vg/mL) was injected slowly (~0.02 µL min-1) by using a Picospritzer (0.2 µL total). After ejection of virus, the micropipette was held in place (5 min) before withdrawal. The scalp was closed with surgical sutures and Vetbond (3M) tissue adhesive and the animal was allowed to recover under analgesia provided by injection of carprofen and buprenorphine SR. After allowing for onset of expression, animals were sacrificed acute slices were harvested.

Electrophysiology

L2/3 PCs were targeted for somatic whole-cell recording in the layer 2/3 region of primary visual cortex by gradient-contrast video microscopy. Electrophysiological recordings were obtained using Multiclamp 700B amplifiers (Molecular Devices). Signals were filtered at 6–10 kHz and sampled at 50 kHz with the Digidata 1440B digitizer (Molecular Devices). For whole-cell recordings, borosilicate patch pipettes (2.5-3.5 MΩ tip resistance) were filled with an intracellular solution containing (in mM) 124 potassium gluconate, 2 KCl, 9 HEPES, 4 $MgCl_2$, 4 NaATP, 3 l-ascorbic acid, and 0.5 NaGTP. Pipette capacitance was neutralized in all recordings and electrode series resistance was compensated using bridge balance in current clamp. Liquid junction potentials were uncorrected.

For cell attached recordings seal resistance of >1GΩ was established, for accurate measurement of action potentials. Cells were held at -80 mV. A stimulating electrode (2.5-3.5 MΩ tip resistance, filled with extracellular solution) was placed in either layer 4 or layer 1 region of the visual cortex, at least 200 µm away from the recorded soma. Stimulation intensities were calibrated to reliably elicit at least 3, but no more than 10 action potentials during the 20 consequent stimuli (50 Hz, 30 s inter-trace intervals, 10-50 µs stimulus length). Stability of the elicited responses was confirmed by an initial 15 repeated measurements. Recordings were post hoc filtered at 2 kHz to remove stimulation artifacts.

Recordings had a series resistance <20 MΩ. Membrane potentials were maintained near –80 mV during current-clamp recordings using constant current bias. AP trains were initiated by somatic current injection (300 ms) normalized to the cellular capacitance in each recording measured immediately in voltage clamp after breakthrough (81). Cellular electrical and firing parameters were established by recording voltage responses to current steps between -6 pA/pF and 20 pA/pF. Sag potential was measured at the -6 pA/pF step, by comparing the negative peak within the first 100 ms of the hyperpolarized voltage response and the mean voltage during the last 50 ms of the stimuli. Input resistance was measured by averaging voltage responses to a 20 pA prepulse current step. Sag ratio was determined as the ratio between the sag amplitude and the steady-state response at the -6 pA/pF current step, except when cells were recorded for measuring neuromodulation (**Fig 7**.), as those experiments were significantly more time-consuming. In these cases, -2 pA/pF current injection was provided.

To establish distance dependent EPSP kinetics, cells were filled with 10 µM Alexa-594. Dendrites were visualized after cell fill with Alexa 594 (10µM) with two-photon laser scanning microscopy using a commercial scan head (Ultima; Bruker Corp) fitted with galvanometer mirrors using a 60x, 1.0 NA objective. The fluorophore was allowed to equilibrate for at least 10 minutes before imaging. The stimulating electrode, filled with extracellular recording solution, was placed in close proximity (<5 µm) of the two-photon visualized dendrite. Stimulation intensity was calibrated to elicit an EPSP with <1 ms delay and approximately 50% failure rate (54.21 ± 8.72%, n= 41). The 50% failure rate was necessary in order to maximize the possibility of stimulating a single input. For L1, L4-Type I, and L4-Type II input stimulations the procedure was the same. Synaptic summation was probed by eliciting 5 consequent responses at 50 Hz. Stimulation intensity was elevated during these recordings to elicit synaptic responses every time for the first stimuli as failures

introduced by lower stimulation intensities can yield inconsistent input activation during the 5 stimuli. Inhibitory blocker SR95531 (10 μM) was only included during signal summation (50 Hz stim) experiments, as our intention was to examine single inputs in an intact system. However, repeated stimuli recruited significant inhibitory components as well, therefore the use of inhibitory blockers was warranted for the uncontaminated analyses of our recordings for the 50Hz repetitive stimulation experiments. Z-stacks were created from the stimulated dendritic region and the connected soma as well for 3D reconstruction in order to establish exact dendritic distances. The group of distal dendritic branches only included a fraction of apical dendrites, however proximal dendrites included both a fraction of apical and basal dendrites, for two reasons; first, basal dendrites are significantly shorter than apical dendrites and our recordings did not include any basal dendrites extending beyond 200 μm, and second, in superficial L2 pyramidal cells classifying dendrites that extend radially into apical or basal classes in ambiguous.

For voltage-clamp recordings, cells were patched in normal extracellular solution to first record their firing patterns. Voltage protocols for I_h current measurements consisted of 300 or 500 ms long voltage steps between −150 and −60 mV. Activation time constant was measured by fitting the initial 100 ms of the current response with a single exponential function. In a subset of recordings CsMeSO4 (2 mM) was bath applied after recording control current responses, to establish cesium-sensitive I_h current kinetics and voltage dependence by subtraction. Series resistances were between 6–20 MΩ (75–80% compensated with 53 μs lag) and were constantly monitored. Data were discarded if the series resistance changed more than 25%.

The dynamic clamp system was built in-house based on a previous publication(82), related online available materials available here: (*http://www.dynamicclamp.com/*). The equations governing the implemented gHCN were identical to those used in the NEURON model construction. Synaptic conductances were built-in predefined conductances available from *http://www.dynamicclamp.com/*.

Intracellular solution perfusion

Intracellular solution was perfused by a custom-built tubing and relay system attached to the pipette holder. Briefly, the pipette was filled with normal intracellular solutions to measure firing patterns and subsequent control measurements of spontaneous and elicited EPSPs. Next, a second intracellular solution was introduced to the pipette through a small tube drilled through the pipette holder, by applying miniscule positive pressure. The intracellular fluid levels were marked before the recording and through a second tube the intracellular solution was siphoned out, to not alter established pipette capacitance. During initial trial experiments using fluorophores in the second intracellular solution it was determined that two minutes is enough for complete exchange of the intracellular solution and intracellular equilibration as well. Data were discarded if the series resistance or pipette capacitance changed more than 20%.

Immunohistochemistry

Two-month-old mice were anesthetized with Nembutal (50mg/mL, i.p.) and perfused transcardially with 4% paraformaldehyde (PFA), 0.05% glutaraldehyde in phosphate buffered saline (PBS). After perfusion, brains were removed from the skull and immersed in 4% PFA overnight at 4°C. Coronal 100 μm-thick sections were then cut on a Vibratome (Leica V1000). Brain slices were permeabilized and incubated in blocking buffer for one hour at room temperature. After blocking, sections were overlaid with primary antibody to HCN1 (1:200, Thermo Fisher Scientific) overnight at 4 °C, then subjected to a 1 h incubation with secondary antibody (Goat anti-Rabbit IgG, 1:200, Thermo Fisher Scientific) at room temperature. Stained sections were mounted with DAPI-containing mounting solution and sealed with glass coverslips. Confocal imaging was carried out on a Leica SP5 MP.

NEURON modeling

Computer simulations were performed using the NEURON simulation environment (versions 7.5 and 7.6, downloaded from *http://neuron.yale.edu*). A constrained NEURON model with an active somatic compartment was downloaded from the publicly available Cell Type Database of the Allen Institute (*http://celltypes.brain-map.org/experiment/electrophysiology/487661754*). Passive properties (axial resistance, specific membrane capacitance and leak conductance density) were altered manually to recreate passive membrane potential responses of whole-cell recorded L2/3 PCs for given stimulus intensities. Both transient and persistent potassium channels were taken out of the model to gain simulation speed as the aim of the simulations was to reproduce subthreshold EPSP dynamics. Final simulations were rerun with intact sodium currents as well to confirm the lack of alterations introduced by these channels. The I_h conductance was based on the built-in Hodgkin–Huxley model of NEURON with freely adjustable sets of parameters(83). I_h model parameters were constrained by our whole-cell voltage clamp recordings. The steady-state activation was governed by the following equation:

$$minf = \frac{1}{1 + e^{\frac{v+21.945}{6.85}}}$$

where v is the local membrane potential. Due to the lack of apparent inactivation, the model operated with a single gate (activation).

The activation and deactivation time constant was defined as

$$mtau = 25.46 * e^{-0.5*\left(\frac{v+100.28}{16.2}\right)^2}$$

To simulate EPSP kinetics, a movable spine (length: 0.6 µm, diameter: 0.6 µm, axial resistance: 150 Ωcm), with spine neck (length: 2 µm, diameter: 0.1 µm, axial resistance: 100 Ωcm) was created. Leak conductance was inserted into both compartments, along with the fitted conductance model. Synaptic inputs were supplemented by using NEURON's built-in AlphaSynapse class. To probe the contribution of specific dendritic conductances to shaping the distance-EPSP halfwidth relationship, selected conductance models were inserted into both apical and basal dendrites with a Gaussian distribution. This curve was selected as modulation of the Gaussian curve's width and y-offset can reproduce a wide variety of feasible distributions such as linear, exponential, or hot-zone-like expression. To model the contribution of dendritic sodium, potassium, and calcium channels to input modulation, NaTs, Kv3_1 and Ca_LVA models were selected. Distribution approximation was done by grid search to avoid local fitting minimums. NMDA receptors were implemented based on a previous publication (84). During the fitting procedure, NMDA activation voltage and AMPA:NMDA ratios were adjusted by a grid search algorithm.

Statistics

Averages of multiple measurements are presented as mean ± SD. Data were statistically analyzed by ANOVA test using Origin software and custom-written Python scripts. Normality of the data was analyzed with Shapira-Wilks test.

Data and software availability

All code used for simulating single and multicompartmental NEURON models will be made available on GitHub and public repositories upon VOR.

Supplementary Figure 1.

ZD-7288 application results in similar active and passive electrical alterations.

a. Representative effect of ZD-7288 on voltage responses to hyperpolarizing current injections. **b.** ZD-7288 abolished sag voltage (0.42 ± 0.07 mV vs 0.1 ± 0.04 mV in control vs ZD-7288 application, respectively, $p=4.5*10^{-4}$, t(15)=4.47, Student's paired-sample t-test, n=16), decreased the resting membrane potential (-75.86 ± 0.84 mV vs -79.73 ± 0.86 mV in control vs ZD-7288 application, respectively, $p=4.41*10^{-4}$, t(15)=4.48, Student's paired-sample t-test, n=16), and increased the input resistance (92.74 ± 6.59 MΩ vs 140.8 ± 13.07 MΩ in control vs ZD-7288 application, respectively, $p=1.79*10^{-4}$, t(15)=-4.93, Student's paired-sample t-test, n=16).

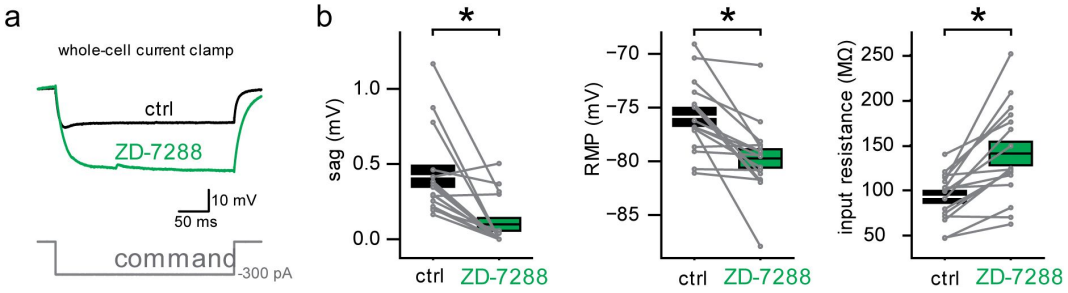

Supplementary Figure 2.

Similar Ih current and effect in different cortical areas.

a. Steady-state rectification of L2/3 PCs in the primary somatosensory cortex (S1), primary motor cortex (M1), primary auditory cortex (A1) and primary visual cortex (V1). **b.** Similar resting membrane potential (left), sag ratio (middle) and input resistance (right) of L2/3 PCs in different cortical areas. **c**. Example hyperpolarization activated current recordings from four cortical areas (left), with similar voltage dependent activation (right).

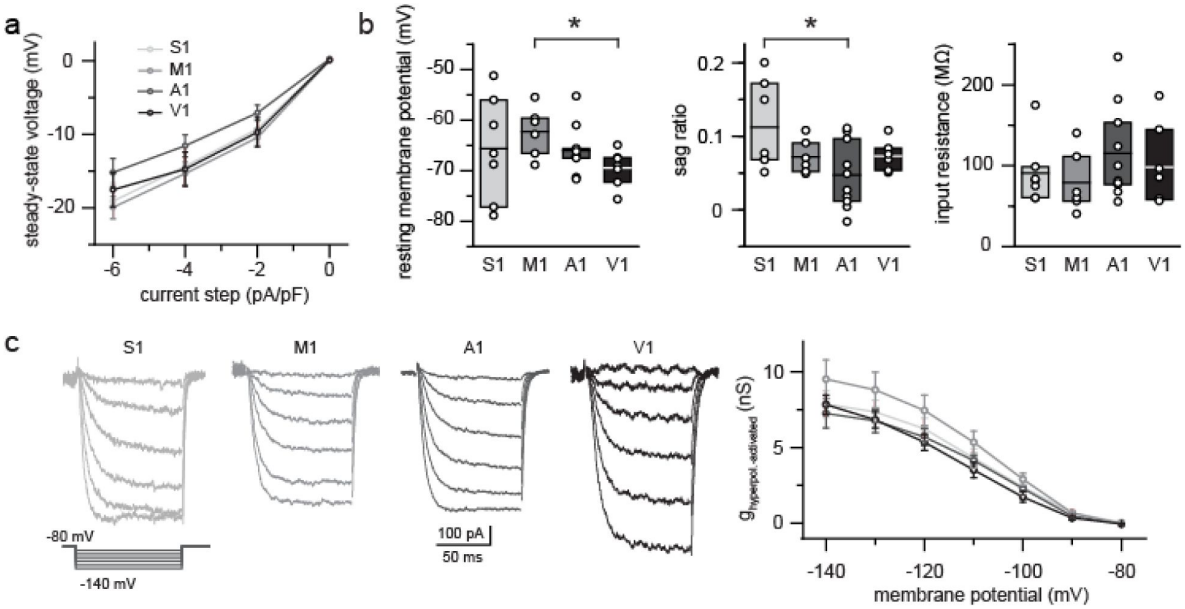

Supplementary Figure 3.

L4-Type I and L4-Type II inputs are well separated by k-means clustering

k-means clustering results plotted along the first and second principal component. Ellipses denote the confidence interval; edges are connected to the cluster center. Hollow circles represent L4 Type II inputs and filled circles represent L4-Type I inputs determined by the experimenter.

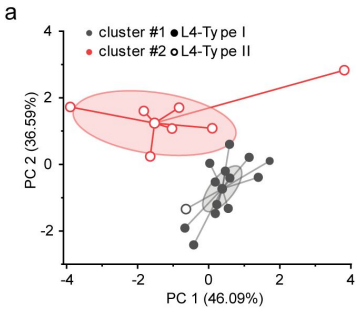

Supplementary Figure 4.

The presence of dendritic sodium and potassium channels cannot explain wider proximal synaptic inputs

a. Sodium channels cannot explain the distance-EPSP halfwidth relationship observed when I_h was blocked. Color coding denotes the ratio between proximal and distal EPSP halfwidths. Notice the miniscule range of the color coding. **C.** Same as panel **b.** but for voltage dependent potassium channels.

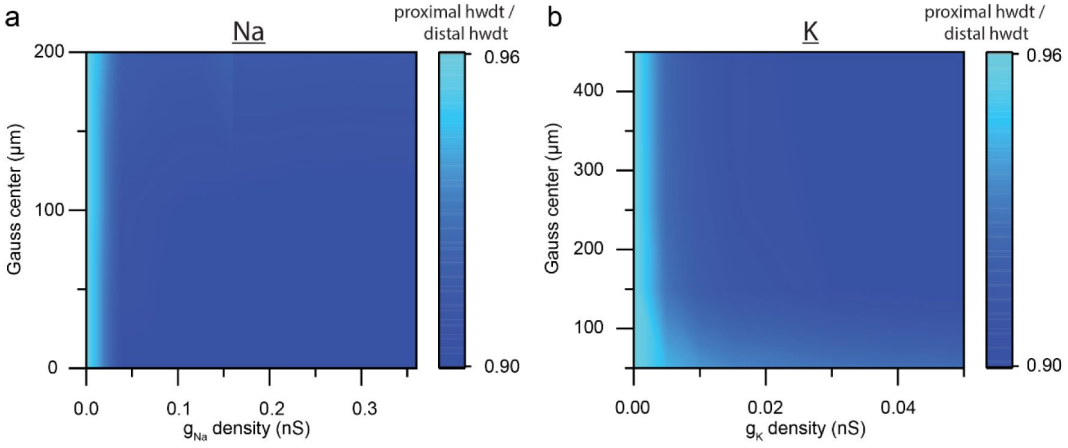

Supplementary Figure 5.

Pipette perfusion does not alter spontaneous circuit activity measurements

a. sEPSP frequency is unaltered by pipette perfusion (6.63 ± 0.3 and 6.4 ± 0.44 for ctrl -80 mV and perfused ctrl -80 mV, p=0.57, t(6) = 0.59, 6.1 ± 0.25 and 6.03 ± 0.33 for ctrl -55 mV and perfused ctrl -55 mV, p=0.83, t(6) = 0.23, n=7 for each, Student's paired-sample t-test). **b.** sEPSP peak amplitudes are stable during pipette perfusion experiments (0.23 ± 0.01 and 0.25 ± 0.01 for ctrl -80 mV and perfused ctrl -80 mV, p=0.43, t(6) = -0.83, 0.16 ± 0.01 and 0.17 ± 0.01 for ctrl prediction and perfused prediction, p=0.43, t(6) =-0.83, 0.31 ± 0.03 and 0.34 ± 0.02 for ctrl -55 mV and perfused ctrl -55 mV, p=0.24, t(6) = -1.31, n=7 each, Student's paired-sample t-test). **c.** Pipette perfusion does not alter measured synaptic amplification (1.92 ± 0.07 and 2.01 ± 0.24 for ctrl and perfused ctrl, p=0.65, t(6) = -0.48, n=7 each, Student's paired-sample t-test).

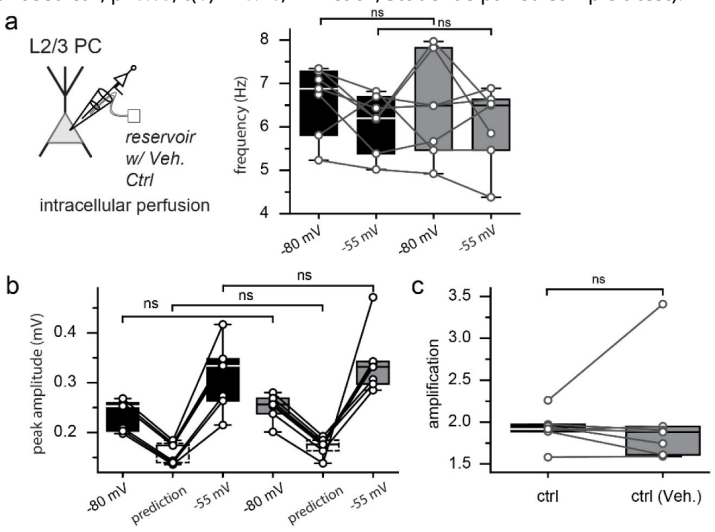

Supplementary Figure 6.

Elicited EPSP halfwidth in not dependent on event amplitude

a. EPSPs elicited by electrical stimulation show no correlation between event amplitude and halfwidth (R^2= 0.021, n=53). **b.** EPSP peak is not dependent on dendritic distance from the soma (R^2= 0.021, n=53).

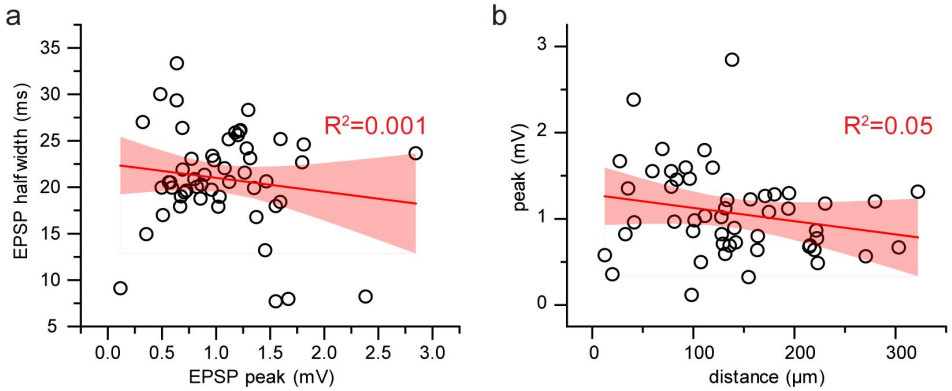

References

1. Quiquempoix M, Fayad SL, Boutourlinsky K, Leresche N, Lambert RC, Bessaih T (2018) **Layer 2/3 pyramidal neurons control the gain of cortical output** *Cell reports* **24**:2799–807

2. Wilson DE, Whitney DE, Scholl B, Fitzpatrick D (2016) **Orientation selectivity and the functional clustering of synaptic inputs in primary visual cortex** *Nature neuroscience* **19**:1003–9

3. Hage TA, Bosma-Moody A, Baker CA, Kratz MB, Campagnola L, Jarsky T, et al. (2022) **Synaptic connectivity to L2/3 of primary visual cortex measured by two-photon optogenetic stimulation** *Elife* **11**

4. Ding Z, Fahey PG, Papadopoulos S, Wang E, Celii B, Papadopoulos C, et al. (2023) **Functional connectomics reveals general wiring rule in mouse visual cortex** *bioRxiv*

5. Scholl B, Wilson DE, Jaepel J, Fitzpatrick D (2019) **Functional logic of layer 2/3 inhibitory connectivity in the ferret visual cortex** *Neuron* **104**:451–7

6. Scholl B, Fitzpatrick D (2020) **Cortical synaptic architecture supports flexible sensory computations** *Current opinion in neurobiology* **64**:41–5

7. Goetz L, Roth A, Häusser M (2021) **Active dendrites enable strong but sparse inputs to determine orientation selectivity** *Proceedings of the National Academy of Sciences* **118**

8. Smith SL, Smith IT, Branco T, Häusser M (2013) **Dendritic spikes enhance stimulus selectivity in cortical neurons in vivo** *Nature* **503**

9. Ujfalussy BB, Makara JK, Lengyel M, Branco T (2018) **Global and multiplexed dendritic computations under in vivo-like conditions** *Neuron* **100**:579–92

10. Landau AT, Park P, Wong-Campos JD, Tian H, Cohen AE, Sabatini BL (2022) **Dendritic branch structure compartmentalizes voltage-dependent calcium influx in cortical layer 2/3 pyramidal cells** *Elife* **11**

11. Ferrarese L, Jouhanneau J-S, Remme MW, Kremkow J, Katona G, Rózsa B, et al. (2018) **Dendrite-specific amplification of weak synaptic input during network activity in vivo** *Cell reports* **24**:3455–65

12. Luo H, Hasegawa K, Liu M, Song W-J (2017) **Comparison of the upper marginal neurons of cortical layer 2 with layer 2/3 pyramidal neurons in mouse temporal cortex** *Frontiers in Neuroanatomy* **11**

13. Stuart GJ, Spruston N (2015) **Dendritic integration: 60 years of progress** *Nature neuroscience* **18**:1713–21

14. Takahashi N, Oertner TG, Hegemann P, Larkum ME (2016) **Active cortical dendrites modulate perception** *Science* **354**

15. Suzuki M, Larkum ME (2020) **General anesthesia decouples cortical pyramidal neurons** *Cell* **180**:666–76

16. Wahl-Schott C, Biel M (2009) **HCN channels: structure, cellular regulation and physiological function** *Cellular and molecular life sciences* **66**:470–94

17. Xu N-l, Harnett MT, Williams SR, Huber D, O'Connor DH, Svoboda K, et al. (2012) **Nonlinear dendritic integration of sensory and motor input during an active sensing task** *Nature* **492**

18. Shah MM (2014) **Cortical HCN channels: function, trafficking and plasticity** *The Journal of physiology* **592**:2711–9

19. Lörincz A, Notomi T, Tamás G, Shigemoto R, Nusser Z (2002) **Polarized and compartment-dependent distribution of HCN1 in pyramidal cell dendrites** *Nature neuroscience* **5**:1185–93

20. Benarroch EE (2013) **HCN channels: function and clinical implications** *Neurology* **80**:304–10

21. Nolan MF, Dudman JT, Dodson PD, Santoro B (2007) **HCN1 channels control resting and active integrative properties of stellate cells from layer II of the entorhinal cortex** *Journal of Neuroscience* **27**:12440–51

22. Kalmbach BE, Buchin A, Long B, Close J, Nandi A, Miller JA, et al. (2018) **h-Channels contribute to divergent intrinsic membrane properties of supragranular pyramidal neurons in human versus mouse cerebral cortex** *Neuron* **100**:1194–208

23. Routh BN, Brager DH, Johnston D (2022) **Ionic and morphological contributions to the variable gain of membrane responses in layer 2/3 pyramidal neurons of mouse primary visual cortex** *Journal of Neurophysiology* **128**:1040–50

24. Datta D, Perone I, Morozov YM, Arellano J, Duque A, Rakic P, et al. (2023) **Localization of PDE4D, HCN1 channels, and mGluR3 in rhesus macaque entorhinal cortex may confer vulnerability in Alzheimer's disease** *Cerebral Cortex*

25. Paspalas CD, Wang M, Arnsten AF (2013) **Constellation of HCN channels and cAMP regulating proteins in dendritic spines of the primate prefrontal cortex: potential substrate for working memory deficits in schizophrenia** *Cerebral cortex* **23**:1643–54

26. Foehring R, Waters R (1991) **Contributions of low-threshold calcium current and anomalous rectifier (Ih) to slow depolarizations underlying burst firing in human neocortical neurons in vitro** *Neuroscience letters* **124**:17–21

27. Bullis JB, Jones TD, Poolos NP (2007) **Reversed somatodendritic Ih gradient in a class of rat hippocampal neurons with pyramidal morphology** *The Journal of physiology* **579**:431–43

28. Williams SR, Stuart GJ (2000) **Site independence of EPSP time course is mediated by dendritic I h in neocortical pyramidal neurons** *Journal of neurophysiology* **83**:3177–82

29. Gouwens NW, Sorensen SA, Baftizadeh F, Budzillo A, Lee BR, Jarsky T, et al. (2020) **Integrated morphoelectric and transcriptomic classification of cortical GABAergic cells** *Cell* **183**:935–53

30. Larkum ME, Waters J, Sakmann B, Helmchen F (2007) **Dendritic spikes in apical dendrites of neocortical layer 2/3 pyramidal neurons** *Journal of Neuroscience* **27**:8999–9008

31. Harnett MT, Magee JC, Williams SR (2015) **Distribution and function of HCN channels in the apical dendritic tuft of neocortical pyramidal neurons** *Journal of Neuroscience* **35**:1024–37

32. Magee JC (1999) **Dendritic Ih normalizes temporal summation in hippocampal CA1 neurons** *Nature neuroscience* **2**:508–14

33. Vetter P, Roth A, Häusser M (2001) **Propagation of action potentials in dendrites depends on dendritic morphology** *Journal of neurophysiology* **85**:926–37

34. Malinow R (1991) **Transmission between pairs of hippocampal slice neurons: quantal levels, oscillations, and LTP** *Science* **252**

35. Yang W, Carrasquillo Y, Hooks BM, Nerbonne JM, Burkhalter A (2013) **Distinct balance of excitation and inhibition in an interareal feedforward and feedback circuit of mouse visual cortex** *Journal of Neuroscience* **33**:17373–84

36. Balcioglu A, Gillani R, Doron M, Burnell K, Ku T, Erisir A, et al. (2023) **Mapping thalamic innervation to individual l2/3 pyramidal neurons and modeling their 'readout'of visual input** *Nature Neuroscience* **26**:470–80

37. Sermet BS, Truschow P, Feyerabend M, Mayrhofer JM, Oram TB, Yizhar O, et al. (2019) **Pathway-, layer- and cell-type-specific thalamic input to mouse barrel cortex** *elife* **8**

38. D'Souza RD, Wang Q, Ji W, Meier AM, Kennedy H, Knoblauch K, et al. (2022) **Hierarchical and nonhierarchical features of the mouse visual cortical network** *Nature communications* **13**

39. Shen S, Jiang X, Scala F, Fu J, Fahey P, Kobak D, et al. (2022) **Distinct organization of two cortico-cortical feedback pathways** *Nature communications* **13**

40. Kondo S, Kiyohara Y, Ohki K (2022) **Response Selectivity of the Lateral Posterior Nucleus Axons Projecting to the Mouse Primary Visual Cortex** *Frontiers in Neural Circuits* **16**

41. Zhuang J, Larsen RS, Takasaki KT, Ouellette ND, Daigle TL, Tasic B, et al. (2019) **The spatial structure of feedforward information in mouse primary visual cortex** *Biorxiv*

42. London M, Hausser M (2005) **Dendritic computation** *Annual review of neuroscience* **28**:503–32

43. Berger T, Senn W, Lüscher H-R (2003) **Hyperpolarization-activated current I h disconnects somatic and dendritic spike initiation zones in layer V pyramidal neurons** *Journal of neurophysiology* **90**:2428–37

44. Tsay D, Dudman JT, Siegelbaum SA (2007) **HCN1 channels constrain synaptically evoked Ca2+ spikes in distal dendrites of CA1 pyramidal neurons** *Neuron* **56**:1076–89

45. Billeh YN, Cai B, Gratiy SL, Dai K, Iyer R, Gouwens NW, et al. (2020) **Systematic integration of structural and functional data into multi-scale models of mouse primary visual cortex** *Neuron* **106**:388–403

46. Palmer LM, Shai AS, Reeve JE, Anderson HL, Paulsen O, Larkum ME (2014) **NMDA spikes enhance action potential generation during sensory input** *Nature neuroscience* **17**:383–90

47. Branco T, Häusser M (2011) **Synaptic integration gradients in single cortical pyramidal cell dendrites** *Neuron* **69**:885–92

48. Bucurenciu I, Kulik A, Schwaller B, Frotscher M, Jonas P (2008) **Nanodomain coupling between Ca2+ channels and Ca2+ sensors promotes fast and efficient transmitter release at a cortical GABAergic synapse** *Neuron* **57**:536–45

49. Cornford JH, Mercier MS, Leite M, Magloire V, Häusser M, Kullmann DM (2019) **Dendritic NMDA receptors in parvalbumin neurons enable strong and stable neuronal assemblies** *Elife* **8**

50. Dodt HU, Frick A, Kampe K, Zieglgänsberger W (1998) **NMDA and AMPA receptors on neocortical neurons are differentially distributed** *European journal of Neuroscience* **10**:3351–7

51. Rowan MJ, Christie JM (2017) **Rapid state-dependent alteration in Kv3 channel availability drives flexible synaptic signaling dependent on somatic subthreshold depolarization** *Cell reports* **18**:2018–29

52. Guet-McCreight A, Chameh HM, Mahallati S, Wishart M, Tripathy SJ, Valiante TA, et al. (2023) **Age-dependent increased sag amplitude in human pyramidal neurons dampens baseline cortical activity** *Cerebral Cortex* **33**:4360–73

53. Santello M, Nevian T (2015) **Dysfunction of cortical dendritic integration in neuropathic pain reversed by serotoninergic neuromodulation** *Neuron* **86**:233–46

54. Dori I, Dinopoulos A, Blue M, Parnavelas J (1996) **Regional differences in the ontogeny of the serotonergic projection to the cerebral cortex** *Experimental neurology* **138**:1–14

55. Vasefi MS, Yang K, Li J, Kruk JS, Heikkila JJ, Jackson MF, et al. (2013) **Acute 5-HT7 receptor activation increases NMDA-evoked currents and differentially alters NMDA receptor subunit phosphorylation and trafficking in hippocampal neurons** *Molecular brain* **6**:1–9

56. Megıas M, Emri Z, Freund T, Gulyas A (2001) **Total number and distribution of inhibitory and excitatory synapses on hippocampal CA1 pyramidal cells** *Neuroscience* **102**:527–40

57. Nevian T, Larkum ME, Polsky A, Schiller J (2007) **Properties of basal dendrites of layer 5 pyramidal neurons: a direct patch-clamp recording study** *Nature neuroscience* **10**:206–14

58. Hubel DH, Wiesel TN (1979) **Brain mechanisms of vision** *Scientific American* **241**:150–63

59. Hubel DH, Wiesel TN (2004) **Brain and visual perception: the story of a 25-year collaboration** Oxford University Press

60. Scholl B, Thomas CI, Ryan MA, Kamasawa N, Fitzpatrick D (2021) **Cortical response selectivity derives from strength in numbers of synapses** *Nature* **590**

61. Waters J, Larkum M, Sakmann B, Helmchen F (2003) **Supralinear Ca2+ influx into dendritic tufts of layer 2/3 neocortical pyramidal neurons in vitro and in vivo** *Journal of Neuroscience* **23**:8558–67

62. Major G, Polsky A, Denk W, Schiller J, Tank DW (2008) **Spatiotemporally graded NMDA spike/plateau potentials in basal dendrites of neocortical pyramidal neurons** *Journal of neurophysiology* **99**:2584–601

63. Harris JA, Mihalas S, Hirokawa KE, Whitesell JD, Choi H, Bernard A, et al. (2019) **Hierarchical organization of cortical and thalamic connectivity** *Nature* **575**

64. Levelt CN, Hübener M (2012) **Critical-period plasticity in the visual cortex** *Annual review of neuroscience* **35**:309–30

65. Bard JA, Zgombick J, Adham N, Vaysse P, Branchek TA, Weinshank RL (1993) **Cloning of a novel human serotonin receptor (5-HT7) positively linked to adenylate cyclase** *Journal of Biological Chemistry* **268**:23422–6

66. Karmarkar UR, Dan Y (2006) **Experience-dependent plasticity in adult visual cortex** *Neuron* **52**:577–85

67. Hensch TK, Bilimoria PM (2012) **Re-opening windows: manipulating critical periods for brain development** *Cerebrum: the Dana forum on brain science*

68. Ogelman R, Gomez Wulschner LE, Hoelscher VM, Hwang I-W, Chang VN, Oh WC (2024) **Serotonin modulates excitatory synapse maturation in the developing prefrontal cortex** *Nature Communications* **15**

69. Nolan MF, Malleret G, Dudman JT, Buhl DL, Santoro B, Gibbs E, et al. (2004) **A behavioral role for dendritic integration: HCN1 channels constrain spatial memory and plasticity at inputs to distal dendrites of CA1 pyramidal neurons** *Cell* **119**:719–32

70. Wu J, El-Hassar L, Datta D, Thomas M, Zhang Y, Jenkins DP, et al. (2023) **Interaction Between HCN and Slack Channels Regulates mPFC Pyramidal Cell Excitability and Working Memory** *bioRxiv*

71. Yu L, Tasaki S, Schneider JA, Arfanakis K, Duong DM, Wingo AP, et al. (2020) **Cortical proteins associated with cognitive resilience in community-dwelling older persons** *JAMA psychiatry* **77**:1172–80

72. Ramírez D, Zúñiga R, Concha G, Zúñiga L (2018) **HCN channels: new therapeutic targets for pain treatment** *Molecules* **23**

73. Ku SM, Han M-H (2017) **HCN channel targets for novel antidepressant treatment** *Neurotherapeutics* **14**:698–715

74. Kim CS, Johnston D (2018) **A possible link between HCN channels and depression** *Chronic Stress* **2**

75. Postea O, Biel M (2011) **Exploring HCN channels as novel drug targets** *Nature reviews Drug discovery* **10**:903–14

76. Lyman KA, Han Y, Chetkovich DM (2017) **Animal models suggest the TRIP8b-HCN interaction is a therapeutic target for major depressive disorder** *Expert Opinion on Therapeutic Targets* **21**:235–7

77. Fukuyama K, Motomura E, Okada M (2023) **Therapeutic potential and limitation of serotonin type 7 receptor modulation** *International Journal of Molecular Sciences* **24**

78. Ishibashi T, Horisawa T, Tokuda K, Ishiyama T, Ogasa M, Tagashira R, et al. (2010) **Pharmacological profile of lurasidone, a novel antipsychotic agent with potent 5-hydroxytryptamine 7 (5-HT7) and 5-HT1A receptor activity** *Journal of Pharmacology and Experimental Therapeutics* **334**:171–81

79. Shimizu M, Mi X, Toyoda F, Kojima A, Ding W-G, Fukushima Y, et al. (2022) **Propofol, an Anesthetic Agent, Inhibits HCN Channels through the Allosteric Modulation of the cAMP-Dependent Gating Mechanism** *Biomolecules* **12**

80. Chen X, Shu S, Kennedy DP, Willcox SC, Bayliss DA (2009) **Subunit-specific effects of isoflurane on neuronal I h in HCN1 knockout mice** *Journal of neurophysiology* **101**:129–40

81. Taylor AL (2012) **What we talk about when we talk about capacitance measured with the voltage-clamp step method** *Journal of computational neuroscience* **32**:167–75

82. Desai NS, Gray R (2017) **Johnston D. A dynamic clamp on every rig** *eneuro* **4**

83. Oláh VJ, Tarcsay G, Brunner J (2021) **Small size of recorded neuronal structures confines the accuracy in direct axonal voltage measurements** *Eneuro* **8**

84. Testa-Silva G, Rosier M, Honnuraiah S, Guzulaitis R, Megias AM, French C, et al. (2022) **High synaptic threshold for dendritic nmda spike generation in human layer 2/3 pyramidal neurons** *Cell reports* **41**

Author information

Viktor János Oláh
Department of Cell Biology, Emory University School of Medicine, Atlanta, United States
ORCID iD: 0000-0002-2069-7525

Jing Wu
Department of Pharmacology, Yale University School of Medicine, New Haven, United States

Leonard K Kaczmarek
Department of Pharmacology, Yale University School of Medicine, New Haven, United States, Department of Cellular and Molecular Physiology, Yale University School of Medicine, New Haven, United States
ORCID iD: 0000-0001-5128-6326

Matthew JM Rowan
Department of Cell Biology, Emory University School of Medicine, Atlanta, United States, Center for Neurodegenerative Disease, Emory University School of Medicine, Atlanta, United States
ORCID iD: 0000-0003-0955-0706

For correspondence: mjrowan@emory.edu

Editors

Reviewing Editor
Helen Scharfman
Nathan Kline Institute, Orangeburg, United States of America

Senior Editor
Panayiota Poirazi
FORTH Institute of Molecular Biology and Biotechnology, Heraklion, Greece

Reviewer #2 (Public review):

Summary:

This paper by Olah et al., uncovers a previously unknown role of HCN channels in shaping synaptic inputs to L2/3 cortical neurons. The authors demonstrate using slice electrophysiology and computational modeling that unlike layer 5 pyramidal neurons, L2/3 neurons have an enrichment of HCN channels in the proximal dendrites. This location provides a locus of neuromodulation for inputs onto the proximal dendrites from L4 without an influence on distal inputs from L1. the authors use pharmacology to demonstrate the effect of HCN channels on NMDA-mediated synaptic inputs from L4. The authors further demonstrate the developmental time course of HCN function in L2/3 pyramidal neurons. Taken together, this a well constructed investigation of HCN channel function and the consequences of these channels on synaptic integration in L2/3 pyramidal neurons.

Strengths:

The authors use careful, well-constrained experiments using multiple pharmacological agents to asses HCN channel contributions to synaptic integrations. The authors also use voltage-clamp to directly measure the current through HCN channels across developmental ages. The authors also provide supplemental data showing that their observation is consistent across multiple areas of the cerebral cortex.

Weaknesses:

The gradient of HCN channel function is based almost exclusively on changes in EPSP width measured at the soma. While providing strong evidence for the presence of HCN current in L2/3 neurons, there are space clamp issues related to the use of somatic whole-cell voltage clamp that should be considered in the discussion. One omission by the authors is related to cell morphology. They make a point of normalizing the current injections to cell capacitance to account for variability in neuronal morphology. It is not clear however, how, if at all, this variability would affect EPSP propagation and modulation by proximal HCN channels. This should at least be discussed. Also, if there is high variability in cell morphology, was this considered in the modeling experiments?

https://doi.org/10.7554/eLife.96002.2.sa2

Reviewer #3 (Public review):

Summary:

The authors study the function of HCN channels in L2/3 pyramidal neurons, employing somatic whole-cell recordings in acute slices of visual cortex in adult mice and a bevy of technically challenging techniques. Their primary claim is a non-uniform HCN distribution across the dendritic arbor with greater density closer to the soma (roughly opposite of the gradient found in L5 PT-type neurons). The second major claim is that multiple sources of long-range excitatory input (cortical and thalamic) are differentially affected by the HCN distribution. They further describe an interesting interplay of NMDAR and HCN, serotonergic modulation of HCN, and compare HCN-related properties at 1-, 2- and 6-weeks of age. Several results are accompanied by biophysical simulations.

Strengths:

The authors collected data from both male and female mice, at an age (6-10 weeks) that permits comparison with in vivo studies, in sufficient numbers for each condition, and they collected a good number of data points for almost all figure panels. This is all the more positive, considering the demanding nature of multi-electrode recording configurations and pipette-perfusion. The main strength of the study is the question and focus.

Weaknesses:

Unfortunately, in its present form, the main claims are not adequately supported by the experimental evidence: primarily because the evidence is indirect and circumstantial, but also because multiple unusual experimental choices (along with poor presentation of results) undermine the reader's confidence. Additionally, the authors overstate the novelty of certain results and fail to cite important related publications. Some of these weaknesses can be addressed by improved analysis, statistics, resolving inconsistent data across figures, reorganizing/improving figure panels, more complete methods, improved citations, and proofreading. In particular, given the emphasis on EPSPs, the primary data (example EPSPs, overlaid conditions) should be shown much more.

However on the experimental side, addressing the reviewer's concerns would require a very substantial additional effort: direct measurement of HCN density at different points in the dendritic arbor and soma; the internal solution chosen here (K-gluconate) is reported to inhibit HCN; bath-applied cesium at the concentrations used blocks multiple potassium channels, i.e. is not selective for HCN (the authors have concerns about using the more selective blocker ZD7288, but did use it in a subset of experiments, some of which show quantitatively different results). In response to initial review, the authors performed pathway-specific synaptic stimulation, via optogenetic activation of specific long-range inputs - this approach is valuable and interesting, however the results are presented very minimally and only partially match those obtained by layer-specific electrical stimulation.

https://doi.org/10.7554/eLife.96002.2.sa1

Author response:

The following is the authors' response to the original reviews.

> ***Public Reviews:***
>
> ***Reviewer #1 (Public Review):***
>
> *The manuscript by Oleh et al. uses in vitro electrophysiology and compartmental modeling (via NEURON) to investigate the expression and function of HCN channels in mouse L2/3 pyramidal neurons. The authors conclude that L2/3 neurons have developmentally regulated HCN channels, the activation of which can be observed when subjected to large hyperpolarizations. They further conclude via blockade experiments that HCN channels in L2/3 neurons influence cellular excitability and pathway-specific EPSP kinetics, which can be neuromodulated. While the authors perform a wide range of slice physiology experiments, concrete evidence that L2/3 cells express functionally relevant HCN channels is limited. There are serious experimental design caveats and confounds that make drawing strong conclusions from the data difficult. Furthermore, the significance of the findings is generally unclear, given modest effect sizes and a lack of any functional relevance, either directly via in vivo experiments or indirectly via strong HCN-mediated changes in known operations/computations/functions of L2/3 neurons.*
>
> *Specific points:*

> *(1) The interpretability and impact of this manuscript are limited due to numerous methodological issues in experimental design, data collection, and analysis. The authors have not followed best practices in the field, and as such, much of the data is ambiguous and/or weak and does not support their interpretations (detailed below). Additionally, the authors fail to appropriately explain their rationale for many of their choices, making it difficult to understand why they did what they did. Furthermore, many important references appear to be missing, both in terms of contextualizing the work and in terms of approach/method. For example, the authors do not cite Kalmbach et al 2018, which performed a directly comparable set of experiments on HCN channels in L2/3 neurons of both humans and mice. This is an unacceptable omission. Additionally, the authors fail to cite prior literature regarding the specificity or lack thereof of Cs+ in blocking HCN. In describing a result, the authors state "In line with previous reports, we found that L2/3 PCs exhibited an unremarkable amount of sag at 'typical' current commands" but they then fail to cite the previous reports.*

We thank the reviewer for the thorough examination of our manuscript; however, we disagree with many of the raised concerns for several reasons, as detailed here:

To address the lack of certain citations, we would like to emphasize that in the introduction section, we did initially focus on the several decades-long line of investigation into the HCN channel content of layer 2/3 pyramidal cells (L2/3 PCs), where there has undoubtedly been some controversy as to their functional contribution. We did not explicitly cite papers that claimed to find no/little HCN channels/sag- although this would be a significant list of publications from some excellent investigators, as methods used may have differed from ours leading to different interpretations. Simply stated, unless one was explicitly looking for HCN in L2/3 PCs, it might go unobserved. However, we now addressed this more clearly in the revision:

Just to take one example: in the publication mentioned by the reviewer (Kalmbach et al 2018), the investigators did not carry out voltage clamp or dynamic clamp recordings, as we did in our work here. Furthermore, the reported input resistance values in the aforementioned paper were far above other reports in mice (Routh et al. 2022, Brandalise et al 2022, Hedrick et al 2012; which were similar to our findings here), suggesting that recordings in Kalmbach were carried out at membrane potentials where HCN activation may be less available (Routh, Brager and Johnston 2022).

Another reason for some mixed findings in the field is undoubtedly due to the small/nonexistent sag in L2/3 current clamp recordings (in mice). We also observed a very small sag, which can be explained by the following: The ‘sag’ potential is a biphasic voltage response emerging from a relatively fast passive membrane response and a slower Ih activation. In L2/3 PCs, hyperpolarization-activated currents are apparently faster than previously described, and are located proximally (Figure 2 & Figure 5). Therefore, their recruitment in mouse L2/3 PCs is on a similar timescale to the passive membrane response, resulting in a more monophasic response. We now include a more full set of citations in the updated introduction section, to highlight the importance of HCN channels in L2/3 PCs in mice (and other species).

The justification for using cesium (i.e., ‘best practices’) is detailed below.

> *(2) A critical experimental concern in the manuscript is the reliance on cesium, a nonspecific blocker, to evaluate HCN channel function. Cesium blocks HCN channels but also acts at potassium channels (and possibly other channels as well). The authors do not acknowledge this or attempt to justify their use of Cs+ and do not cite prior work on this subject. They do not show control experiments demonstrating that the application of Cs+ in their preparation only affects Ih. Additionally, the authors write 1 mM cesium in the*

> *text but appear to use 2 mM in the figures. In later experiments, the authors switch to ZD7288, a more commonly used and generally accepted more specific blocker of HCN channels. However, they use a very high concentration, which is also known to produce off-target effects (see Chevaleyre and Castillo, 2002). To make robust conclusions, the authors should have used both blockers (at accepted/conservative concentrations) for all (or at least most) experiments. Using one blocker for some experiments and then another for different experiments is fraught with potential confounds.*

To address the concerns regarding the usage of cesium to block HCN channels, we would like to state that neither cesium nor ZD-7288 are without off-target effects, however in our case the potential off-target effects of external cesium were deemed less impactful, especially concerning AP firing output experiments. Extracellular cesium has been widely accepted as a blocker of HCN channels (Lau et al. 2010, Wickenden et al. 2009, Rateau and Ropert 2005, Hemond et al. 2009, Yang et al. 2015, Matt et al. 2010). However, it is well known to act on potassium channels as well at higher concentrations, which has been demonstrated with intracellular and extracellular application (Puil et al. 1981, Fleidervish et al. 2008, Williams et al. 1991, 2008).

Although we initially performed 'internal' control experiments to ensure the cesium concentration was unlikely to greatly block voltage gated K+ channels during our recordings, we recognize these were not included in the original manuscript. These are detailed as follows: during our recordings cesium had no significant effect on action potential halfwidth, ruling out substantial blocking of potassium channels, nor did it affect any other aspects of suprathreshold activity (now reported in results, page 4 - line 113). Furthermore, we observed similar effects on passive properties (resting membrane potential, input resistance) following ZD-7288 as with cesium, which we now also updated in our figures (Supplementary Figure 1). We did acknowledge that ZD-7288 is a widely accepted blocker of HCN, and for this reason we carried out some of our experiments using this pharmacological agent instead of cesium.

On the other hand, ZD-7288 suffers from its own side effects, such as potential effects on sodium channels (Wu et al. 2012) and calcium channels (Sánchez-Alonso et al. 2008, Felix et al. 2003). As our aim was to provide functional evidence for the importance of HCN channels, we initially deemed these potential effects unacceptable in experiments where AP firing output (e.g., in cell-attached experiments) was measured. Nonetheless, in new experiments now included here, we found the effects of ZD and cesium on AP output were similar as shown in new Supplemental Figure 1.

Many experiments were supported by complementary findings using external cesium and ZD-7288. For example, the effect of ZD-7288 on EPSPs was confirmed by similar synaptic stimulation experiments using cesium. This is important, as synaptic inputs of L2/3 PCs are modulated by both dendritic sodium (Ferrarese et al. 2018) and calcium channels (Landau 2022), therefore the application of ZD-7288 alone may have been difficult to interpret in isolation. We thank the reviewer for bringing up this important point.

> *(3) A stronger case could be made that HCN is expressed in the somatic compartment of L2/3 cells if the authors had directly measured HCN-isolated currents with outside-out or nucleated patch recording (with appropriate leak subtraction and pharmacology). Whole-cell voltage-clamp in neurons with axons and/or dendrites does not work. It has been shown to produce erroneous results over and over again in the field due to well-known space clamp problems (see Rall, Spruston, Williams, etc.). The authors could have also included negative controls, such as recordings in neurons that do not express HCN or in HCN-knockout animals. Without these experiments, the authors draw a false equivalency between the effects of cesium and HCN channels, when the outcomes they describe could be driven simply by multiple other cesium-sensitive currents. Distortions*

> *are common in these preparations when attempting to study channels (see Williams and Womzy, J Neuro, 2011). In Fig 2h, cesium-sensitive currents look too large and fast to be from HCN currents alone given what the authors have shown in their earlier current clamp data. Furthermore, serious errors in leak subtraction appear to be visible in Supplementary Figure 1c. To claim that these conductances are solely from HCN may be misleading.*

We disagree with the argument that "Whole-cell voltage-clamp in neurons with axons and/or dendrites does not work". Although this method is not without its confounds (i.e. space clamp), it is still a useful initial measure as demonstrated countless times in the literature. However, the reviewer is correct that the best approach to establish the somatodendritic distribution of ion channels is by direct somatic and dendritic outside-out patches. Due to the small diameter of L2/3 PC dendrites, these experiments haven't been carried out yet in the literature for any other ion channel either to our knowledge. Mapping this distribution electrophysiologically may be outside the scope of the current manuscript, but it was hard for us to ignore the sheer size of the Cs^+ sensitive hyperpolarizing currents in whole cell. Thus, we will opt to report this data.

Also, we should point out that space clamp-related errors manifest in the overestimation of frequency-dependent features, such as activation kinetics, and underestimation of steady-state current amplitudes. The activation time constant of our measured currents are somewhat faster than previously reported; reducing major concerns regarding space clamp errors. Furthermore, we simply do not understand what "too large… to be from HCN currents" means. Our voltage-clamp measured currents are similar to previously reported HCN currents (Meng et al. 2011, Li 2011, Zhao et al. 2019, Yu et al. 2004, Zhang et al. 2008, Spinelli et al. 2018, Craven et al. 2006, Ying et al. 2012, Biel et al. 2009).

Furthermore, we should point out that our measured currents activated at hyperpolarized voltages, had the same voltage dependence as HCN currents, did not show inactivation, influenced both input resistance and resting membrane potential, and are blocked by low concentration extracellular cesium. Each of these features would point to HCN.

> *(4) The authors present current-clamp traces with some sag, a primary indicator of HCN conductance, in Figure 2. However, they do not show example traces with cesium or ZD7288 blockade. Additionally, the normalization of current injected by cellular capacitance and the lack of reporting of input resistance or estimated cellular size makes it difficult to determine how much current is actually needed to observe the sag, which is important for assessing the functional relevance of these channels. The sag ratio in controls also varies significantly without explanation (Figure 6 vs Figure 7). Could this variability be a result of genetically defined subgroups within L2/3? For example, in humans, HCN expression in L2/3 varies from superficial and deep neurons. The authors do not make an effort to investigate this. Regardless of inconsistencies in either current injection or cell type, the sag ratio appears to be rather modest and similar to what has already been reported previously in other papers.*

We thank the reviewer for pointing out that our explanation for the modest sag ratio might have not been sufficient to properly understand why this measurement cannot be applied to layer 2/3 pyramidal cells. Briefly: sag potential emerges from a relatively (compared to I_h) fast passive membrane response and a slower HCN recruitment. The opposing polarity and different timescales of these two mechanisms results in a biphasic response called "sag" potential. However, if the timescale of these two mechanisms is similar, the voltage response is not predicted to be biphasic. We have shown that hyperpolarization activated currents in our preparations are fast and proximal, therefore they are recruited during the passive response (see Figure 2g.). This means that although a substantial amount of HCN currents are activated during hyperpolarization, their activation will not result in substantial sag.

Therefore, sag ratio measurement is not necessarily applicable to approximate the HCN content of mouse L2/3 PCs. We would like to emphasize that sag ratio measurements *are correct in case of other cell types* (i.e. L5 and CA1 PCs_,_ and our aim is not to discredit the method, but rather to show that it cannot be applied similarly in the case of mouse L2/3 PCs.

Our own measurements, similar to others in the literature show that L2/3 PCs exhibit modest sag ratios, however, this does not mean that HCN is not relevant. I_h activation in L2/3 PCs does not manifest in large sag potential but rather in a continuous distortion of steady-state responses (Figure 2b.). The reviewer is correct that L2/3 PCs are non-homogenous, therefore we sampled along the entire L2/3 axis. This yielded some potential variability in our results (i.e., passive properties); yet we did not observe any cells where hyperpolarizing-activated/Cs^+-sensitive currents could not be resolved. As structural variability of L2/3 cells does result in variability in cellular capacitance, we compensated for this variability by injecting cellular capacitance-normalized currents. Our measured cellular capacitances were in accordance with previously published values, in the range of 50-120 pF. Therefore, the injected currents were not outside frequently used values. Together, we would like to state that whether substantial sag potential is present or not, initial estimates of the HCN content for each L2/3 PC should be treated with caution.

> *(5) In the later experiments with ZD7288, the authors measured EPSP half-width at greater distances from the soma. However, they use minimal stimulation to evoke EPSPs at increasingly far distances from the soma. Without controlling for amplitude, the authors cannot easily distinguish between attenuation and spread from dendritic filtering and additional activation and spread from HCN blockade. At a minimum, the authors should share the variability of EPSP amplitude versus the change in EPSP half-width and/or stimulation amplitudes by distance. In general, this kind of experiment yields much clearer results if a more precise local activation of synapses is used, such as dendritic current injection, glutamate uncaging, sucrose puff, or glutamate iontophoresis. There are recording quality concerns here as well: the cell pictured in Figure 3a does not have visible dendritic spines, and a substantial amount of membrane is visible in the recording pipette. These concerns also apply to the similar developmental experiment in 6f-h, where EPSP amplitude is not controlled, and therefore, attenuation and spread by distance cannot be effectively measured. The outcome, that L2/3 cells have dendritic properties that violate cable theory, seems implausible and is more likely a result of variable amplitude by proximity.*

To resolve this issue, we made a supplementary figure showing elicited amplitudes, which showed no significant distance dependence and minimal variability (new Supplementary Figure 6). We thank the reviewer for suggesting an amplitude-halfwidth comparison control (now included as new Supplementary Figure 6).). To address the issue of the non-visible spines, we would like to note that these images are of lower magnification and power to resolve them. The presence of dendritic spines was confirmed in every recorded pyramidal cell observed using 2P microscopy at higher magnification.

We would like to emphasize that although our recordings “seemingly” violated the cable theory, this is only true if we assume a completely passive condition. As shown in our manuscript, cable theory was not violated, as the presence of NMDA receptor boosting explained the observed ‘non-Rallian’ phenomenon.

> *(6) Minimal stimulation used for experiments in Figures 3d-i and Figures 4g-h does not resolve the half-width measurement's sensitivity to dendritic filtering, nor does cesium blockade preclude only HCN channel involvement. Example traces should be shown for all conditions in 3h; the example traces shown here do not appear to even be from the same cell. These experiments should be paired (with and without cesium/ZD). The same problem appears in Figure 4, where it is not clear that the authors performed controls*

> *and drug conditions on the same cells. 4g also lacks a scale bar, so readers cannot determine how much these measurements are affected by filtering and evoked amplitude variability. Finally, if we are to believe that minimal stimulation is used to evoke responses of single axons with 50% fail rates, NMDA receptor activation should be minimal to begin with. If the authors wish to make this claim, they need to do more precise activation of NMDA-mediated EPSPs and examine the effects of ZD7288 on these responses in the same cell. As the data is presented, it is not possible to draw the conclusion that HCN boosts NMDA-mediated responses in L2/3 neurons.*

As stated in the figure legends, the control and drug application traces are from the same cell, both in figure 3 and figure 4, and the scalebar is not included as the amplitudes were normalized for clarity. We have address the effects of dendritic filtering above in answer (5), and cesium blockade above in answer (2). To reiterate, dendritic filtering alone cannot explain our observations, and cesium is often a better choice for blocking HCN channels compared to ZD-7288, which blocks sodium channels as well.

When an excitatory synaptic signal arrives onto a pyramidal cell in typical conditions, neurotransmitter sensitive receptors transmit a synaptic current to the dendritic spine. This dendritic spine is electrically isolated by the high resistance of the spine neck and due to the small membrane surface of the spine, the synaptic current can elicit remarkably large voltage changes. These voltage changes can be large enough to depolarize the spine close to zero millivolts upon even single small inputs (Jayant et al. 2016). Therefore, to state that single inputs arriving to dendritic spines cannot be large enough to recruit NMDA receptor activation is incorrect. This is further exemplified by the substantial literature showing 'miniature' NMDA recruitment via stochastic vesicle release alone.

> *(7) The quality of recordings included in the dataset has concerning variability: for example, resting membrane potentials vary by >15-20 mV and the AP threshold varies by 20 mV in controls. This is indicative of either a very wide range of genetically distinct cell types that the authors are ignoring or the inclusion of cells that are either unhealthy or have bad seals.*

Although we are aware of the diversity of L2/3 PCs, resolving further layer depth differences is outside the scope of our current manuscript. However, as shown in Kalmbech et al, resting membrane potential can greatly vary (>15-20 mV) in L2/3 PCs depending on distance from pia. We acknowledge that the variance in AP threshold is large and could be due to genetically distinct cell types.

> *(8) The authors make no mention of blocking GABAergic signaling, so it must be assumed that it is intact for all experiments. Electrical stimulation can therefore evoke a mixture of excitatory and inhibitory responses, which may well synapse at very different locations, adding to interpretability and variability concerns.*

We thank the reviewer for pointing out our lack of detail regarding the GABAergic signaling blocker SR 95531. We did include this drug in our recordings of (50Hz stim.) signal summation, so GABAergic responses did not contaminate our recordings. We now included this information in the results section (page 5) and the methods section (page 15)

> *(9) The investigation of serotonergic interaction with HCN channels produces modest effect sizes and suffers the same problems as described above.*

We do not agree with the reviewer that 50% drop in neuronal AP firing responses (Figure 7b) was a modest effect size. Thus, we opted to keep this data in the manuscript.

> *(10) The computational modeling is not well described and is not biologically plausible. Persistent and transient K channels are missing. Values for other parameters are not listed. The model does not seem to follow cable theory, which, as described above, is not only implausible but is also not supported by the experimental findings.*

The model was downloaded from the Cell Type Database from the Allen Institute, with only minor modifications including the addition of dendritic HCN channels and NDMA receptors-which were varied along a wide parameter space to find a 'best fit' to our observations. These additions were necessary to recapitulate our experimental findings. We agree the model likely does not fully recapitulate all aspects of the dendrites, which as we hope to convey in this manuscript, are not fully resolved in mouse L2/3 PCs. This is a previously published neuronal model, and despite its potential shortcomings, is one among a handful of open-source neuronal models of a fully reconstructed L2/3 PC.

> ***Reviewer #2 (Public Review):***
>
> *Summary:*
>
> *This paper by Olah et al. uncovers a previously unknown role of HCN channels in shaping synaptic inputs to L2/3 cortical neurons. The authors demonstrate using slice electrophysiology and computational modeling that, unlike layer 5 pyramidal neurons, L2/3 neurons have an enrichment of HCN channels in the proximal dendrites. This location provides a locus of neuromodulation for inputs onto the proximal dendrites from L4 without an influence on distal inputs from L1. The authors use pharmacology to demonstrate the effect of HCN channels on NMDA-mediated synaptic inputs from L4. The authors further demonstrate the developmental time course of HCN function in L2/3 pyramidal neurons. Taken together, this a well-constructed investigation of HCN channel function and the consequences of these channels on synaptic integration in L2/3 pyramidal neurons.*
>
> *Strengths:*
>
> *The authors use careful, well-constrained experiments using multiple pharmacological agents to asses HCN channel contributions to synaptic integrations. The authors also use a voltage clamp to directly measure the current through HCN channels across developmental ages. The authors also provide supplemental data showing that their observation is consistent across multiple areas of the cerebral cortex.*
>
> *Weaknesses:*
>
> *The gradient of the HCN channel function is based almost exclusively on changes in EPSP width measured at the soma. While providing strong evidence for the presence of HCN current in L2/3 neurons, there are space clamp issues related to the use of somatic whole-cell voltage clamps that should be considered in the discussion.*

We thank the reviewer for pointing out our careful and well-constrained experiments and for making suggestions. The potential effects of space clamp errors are detailed in the extended explanations under Reviewer 1, Specific points (3).

> ***Reviewer #3 (Public Review):***
>
> *Summary:*
>
> *The authors study the function of HCN channels in L2/3 pyramidal neurons, employing somatic whole-cell recordings in acute slices of visual cortex in adult mice and a bevy of technically challenging techniques. Their primary claim is a non-uniform HCN*

> *distribution across the dendritic arbor with a greater density closer to the soma (roughly opposite of the gradient found in L5 PT-type neurons). The second major claim is that multiple sources of long-range excitatory input (cortical and thalamic) are differentially affected by the HCN distribution. They further describe an interesting interplay of NMDAR and HCN, serotonergic modulation of HCN, and compare HCN-related properties at 1, 2 and 6 weeks of age. Several results are supported by biophysical simulations.*
>
> *Strengths:*
>
> *The authors collected data from both male and female mice, at an age (6-10 weeks) that permits comparison with in vivo studies, in sufficient numbers for each condition, and they collected a good number of data points for almost all figure panels. This is all the more positive, considering the demanding nature of multi-electrode recording configurations and pipette-perfusion. The main strength of the study is the question and focus.*
>
> *Weaknesses:*
>
> *Unfortunately, in its present form, the main claims are not adequately supported by the experimental evidence: primarily because the evidence is indirect and circumstantial, but also because multiple unusual experimental choices (along with poor presentation of results) undermine the reader's confidence. Additionally, the authors overstate the novelty of certain results and fail to cite important related publications. Some of these weaknesses can be addressed by improved analysis and statistics, resolving inconsistent data across figures, reorganizing/improving figure panels, more complete methods, improved citations, and proofreading. In particular, given the emphasis on EPSPs, the primary data (for example EPSPs, overlaid conditions) should be shown much more.*
>
> *However, on the experimental side, addressing the reviewer's concerns would require a very substantial additional effort: direct measurement of HCN density at different points in the dendritic arbor and soma; the internal solution chosen here (K-gluconate) is reported to inhibit HCN; bath-applied cesium at the concentrations used blocks multiple potassium channels, i.e. is not selective for HCN (the fact that the more selective blocker ZD7288 was used in a subset of experiments makes the choice of Cs+ as the primary blocker all the more curious); pathway-specific synaptic stimulation, for example via optogenetic activation of specific long-range inputs, to complement / support / verify the layer-specific electrical stimulation.*

We thank the reviewer for their very careful examination of our manuscript and helpful suggestions. We addressed the concerns raised in the review and presented more raw traces in our figures. Although direct dendritic HCN mapping measurements are outside the scope of the current manuscript due to the morphological constraints presented by L2/3 PCs (which explains why no other full dendritic nonlinearity distribution has been described in L2/3 PCs with this method), we nonetheless supplemented our manuscript with additional suggested experiments as suggested. For example, we included the excellent suggestion of pathway-specific optogenetic stimulation to further validate the disparate effect of HCN channels for distal and proximal inputs. We agree that ZD-7288 is a widely accepted blocker of HCN channels. However, the off-target effects on sodium channels may have significantly confounded our measurements of AP output using extracellular stimulation. Therefore, we chose low concentration cesium as the primary blocker for those experiments, but now validated several other Cs^+-based results with ZD-7288 as well.

> ***Recommendations for the authors:***

> ***Reviewer #2 (Recommendations For The Authors):***
>
> *I have some issues that need clarification or correction.*
>
> *(1) On page 3, line 90, the authors state "We found that bath application of Cs+ (1mM)..." but the methods and Figure 1 state "2mM Cs+". Please check and correct.*

Correct, typo corrected.

> *(2) Related to Cs+ application, the methods state that "CsMeSO4 (2mM) was bath applied..." Is this correct? CsMeSO4 is typically used intracellularly while CsCl is used extracellularly. If so, please justify. If not, please correct.*

It is correct. The justification for not using CsCl selectively extracellularly is that introducing intracellular chloride ions can significantly alter basic biophysical properties, unrelated to the cesium effect. However, no similar distinction has been made for CsMeSO4, which would exclude the use of this drug extracellularly.

> *(3) The authors normalize the current injections by cell capacitance (pA/pF). Was this done because there is a significant variance in cell morphology? A bit of justification for why the authors chose to normalize the current injection this way would help. If there is significant variation in cell capacitance across cells (or developmental ages), the authors could also include these data.*

Indeed, we choose to normalize current injection to cellular capacitance due to the markedly different morphology of deep and superficial L2/3 PCs. Deeper L2/3 PCs have a pronounced apical branch, closely resembling other pyramidal cell types such as L5 PCs, while superficial L2/3 PC lack a thick main apical branch and instead are equipped with multiple, thinner apical dendrites. This morphological variation would yield an inherent bias in several of the reported measurements, therefore we corrected for it by normalizing current injection to cellular capacitance, similar to our previous recent publications (Olah, Goettemoeller et al., 2022, Goettemoeller et al. 2024, Kumar et al. 2024).

> *(4) On page 15, line 445, the section heading is "PV cell NEURON modeling". Is this a typo? The models are of L2/3 pyramidal neurons, correct?*

Correct, typo corrected.

> *(5) Figures 3F and 3I are plots of the voltage integral for different inputs before and after Cs+. The y-axis label units are "pA*ms". This should be "mV*ms" for a voltage integral.*

Correct, typo corrected.

> *(6) On page 9, line 273, the text reads "Voltage clamp experiments revealed that the rectification of steady-state voltage responses to hyperpolarizing current injection was amplified with 5-CT (Fig. 7c)". Both the text and Figure 7C describe current clamp, not voltage clamp, recordings. Please check and correct.*

Correct, typo corrected.

> *(7) Figure 2i looks to be a normalized conductance vs voltage (i.e. activation) plot. The y-axis shows 0-1 but the units are in nS. Is that a coincidence or an error?*

Correct, typo corrected.

> ***Reviewer #3 (Recommendations For The Authors)**:*
>
> *This is your paper. My comments are my own opinion, I don't expect you to agree or to respond. But I hope that what I wrote below will help you to understand my perspective.*
>
> *Please pardon my directness (and sheer volume) in this section - I have a lot of notes/thoughts and hope you may find some of them helpful. My high-level comments are unfortunately rather critical, and in (small) part that is because I encountered too many errors/typos/ambiguities in figures, legend, and text. I expect many would be caught with good proofreading, but uncorrected caused confusion on my part, or an inability to interpret your figures with confidence, given some ambiguity.*
>
> *The paper reads a bit like patchwork - likely a result of many "helpful" reviewers who came before me. Consider starting with and focusing on the synaptic findings, expanding the number of figures and panels dedicated to that, showing example traces for all conditions, and giving yourself the space to portray these complex experiments and results. While I'm not a fan of a large number of supplemental figures, I feel you could move the "extra" results to the supplementals to improve the focus and get right to the meat of it.*
>
> *For me, the main concern is that the evidence you present for the non-uniform HCN distribution is rather indirect. Ideally, I'd like to see patch recordings from various dendritic locations (as others have done in rats, at least; I'm not sure if L2/3 mice have had such conductance density measurements made in basal and apical dendrites). Otherwise, perhaps optical mapping, either functional or via staining. I also mention some concerns about the choice of internal and cesium. More generally, I want to see more primary data (traces), in particular for the big synaptic findings (non-uniform, L1-vs-L4 differences, NMDAR).*

We thank the reviewer for the helpful suggestions. Indeed, direct patch clamp recording is widely considered to be the best method to identify dendritic ion channel distribution, however, we choose an *in silico* approach instead, for several reasons. Undoubtedly, one of the main reasons to omit direct dendritic recordings was that due to the uniquely narrow apical dendrites this method is extremely challenging, with no previous examples in the literature where isolated dendritic outside-out patch recordings were achieved from this cell type. However, there are theoretical considerations as well. In primates, it has been demonstrated that HCN1 channels are concentrated on dendritic spines (Datta et al., 2023) therefore direct outside-out recordings are not adequate in these circumstances. In future experiments we could directly target L2/3 PC dendrites for outside out recordings in order to resolve dendritic nonlinearity distribution, although a cell-attached methodology may be better suited due to the HCN biophysical properties being closely regulated by intracellular signaling pathways.

> *The introduction and Figures 1 and 2 are not so interesting and not entirely accurate: L2/3 do not have "abundant" HCN, nor is there an actual controversy about whether they have HCN. It's been clear (published) for years that they have about the same as all other non-PT neocortical pyramidal neurons (see e.g. Larkum 2007; Sheets 2011). Your own Figure 1A has a logarithmic scale and shows L2/3 as having the lowest expression (?) of all pyramidals and roughly 10x lower than L5 PT, but the text says "comparable", which is misleading.*

We thank the reviewer for this comment. Although there are sporadic reports in the literature about the HCN content of L2/3 PCs, most of these publications arrive to the same conclusion from the negligible sag potential (as the mentioned Larkum et al., 2007

publication); namely that L2/3 PCs do not contain significant amount of HCN channels. We have shown with voltage and current clamp recordings that this assumption is false, as sag potential is not a reliable indicator of HCN content in L2/3 PCs. With the term “controversial” we aimed to highlight the different conclusions of functional investigations (e.g. Sheets et al., 2011) and sag potential recordings (e.g. Larkum et al., 2007), regarding the importance of HCN channels in L2/3 PCs.

> *Non-uniform HCN with distal lower density has already been published for a (rare) pyramidal neuron in CA1 (Bullis 2007), similar to what you found in L2/3, and different from the main CA1 population.*

We thank the reviewer for this suggestion. We have now included the mentioned citation in the introduction section (page 3).

> *Express sag as a ratio or percentage, consistently. Figure out why in Figure 7 the average sag ratio is 0.02 while in Fig. S1 it is 0.07 (for V1) - that is a massive difference.*

The calculation of sag ratio is consistent across the manuscript (at -6pA.pF), except for experiments depicted in Fig. 7 where sag ratio was calculated from -2pA/pF steps. Explanation below:

> *Sag should be measured at a common membrane potential, with each neuron receiving a current pulse appropriate to reach that potential. Your approach of capacitance-based may allow for the same, but it is not clear which responses are used to calculate a single sag value per cell (as in Figure 2d).*

Thank you, we now included this info in the methods section. Sag potential was measured at the -6 pA/pF step peak voltage, except for Fig. 7 as noted above. We have now included this discrepancy detail in the methods section (page 14). These recordings in Fig. 7 took significantly longer than any other recording in the manuscript, as it took a considerable time to reach steady-state response from 5-CT application. -6pA/pF is a current injection in the range of 400-800 pA, which was proven to be too severe for continued application in cells after more than an hour of recording. Accordingly, we decided to lower the hyperpolarizing current step in these recordings. The absolute value of sag is thus different in Fig. 7, but nonetheless the 5-CT effect was still significant. Notably, we probably wouldn’t have noticed the small sag in L2/3 here (and thus the entire study), save for the fact that we looked at -6pA/pF to begin.

> *In a paper focused on HCN, I would have liked to see resonance curves in the passive characterization.*

We thank the reviewer for the suggestion. Resonance curves can indeed provide useful insights into the impact of HCN on a cell’s physiological behavior, however, these experiments are outside the scope of our current manuscript as without *in vivo* recordings, resonance curves do not contribute to the manuscript in our opinion.

> *How did you identify L2/3? Did you target cells in L2 or L3 or in the middle, or did you sample across the full layer width for each condition? A quantitative diagram showing where you patched (soma) and where you stimulated (L1, L4) with actual measurements, would be helpful (supplemental perhaps). You mention in the text that some L2/3 don't have a tuft, suggesting some variability in morphology - some info on this would be useful, i.e. since you did fill at least some of the neurons (eg 3A), how similar/different are the dendritic arbors?*

We sampled the entire L2/3 region during our recordings. It has been published that deep and superficial L2/3 PCs are markedly different in their morphology, and a recent publication (Brandelise et al. 2023) has even separated these two subpopulations to broad-tufted and slender tufted pyramidal cells, which receive distinct subcortical inputs. Although this differentiation opens exciting avenues for future research, examining potential layer gradients in our dataset would warrant significantly higher sample numbers and is currently out of the scope of our manuscript.

> *Distal vs proximal: this could use more clarification, considering how central it is to your results. What about a synapse on a basal dendrite, but 150 or 200 um from the soma, is that considered proximal? Is the distance to the soma you report measured along the 3D dendrite, along the 2D dendrite, as a straight line to the soma, or just relative to some layers or cortical markers? (I apologize if I missed this).*

We thank the reviewer for pointing out the missing description in the results section. We have amended this oversight (p15). Furthermore, although deeper L3 PCs have characteristic apical and basal dendritic branches, when recordings were made from more superficial L2 cells, a large portion of their dendrites extended radially, which made their classification ambiguous. Therefore, we did not use “apical” and “basal” terminology in the paper to avoid confusion. Distances were measured along the 3D reconstructed surface of the recovered pyramidal cells. This information is now included in the methods.

> *Line 445, "PV cell NEURON modeling" ... hmm. Everyone re-uses methods sections to some degree, but this is not confidence-inspiring, and also not from a proofreading perspective.*

We have corrected the typo.

> *It seems that you constructed a new HCN NEURON mechanism when several have been published/reviewed already. Please explain your reasons or at least comment on the differences.*

There are slight differences in our model compared to previously published models. Nevertheless, we took a previously published HCN model as a base (Gasparini et al, 2004), and created our own model to fit our whole-cell voltage clamp recordings.

> *Bath-applied Cs+ can change synaptic transmission (in the hippocampus; Chevaleyre 2002). But also ZD7288 has some such effects. Also, see (Harris 1995) for a Cs+ and ZD7288 comparison. As well as (Harris 1994) for more Cs+ side-effects (it broadens APs, etc). Bath-applied blockers may affect both long-range and local synapses in your recordings, via K-channels or perhaps presynaptic HCN (though I am aware of your Fig. 1e). Since you can do intracellular perfusion, you could apply ZD7288 postsynaptically (Sheets 2011), an elegant solution.*

We thank the reviewer for the suggestion. We were aware of the potential presynaptic effects of cesium (i.e., presynaptic Kv or other channel effects) and did measure PPR after cesium application (Fig. 1h), noting no effect. At Cs^+ concentrations used here, we now also include new data in the results showing no effect on somatically recorded AP waveform (i.e., representative of a Kv channel effect). As stated earlier for reviewer 1, we now performed additional experiments using either cesium or ZD-7288 for comparison (e.g., see updated Fig. 1; Supplementary Figure 1; Fig. 3b-e). Intracellular ZD re-perfusion is an elegant solution which we will absolutely consider in future experiments.

> *K-Gluconate is reported to inhibit Ih (Velumian 1997), consider at least some control experiments with a different internal for the main synaptic finding - maybe you'll find no big change ...*

We thank the reviewer for the suggestion. Although K-Gluconate can inhibit HCN current, the use of this intracellular solution is often used in the literature to measure this current (Huang & Trussel 2014). We have chosen this intracellular solution to improve recording stability.

> *(Biel 2009) is a very comprehensive HCN review, you may find it useful.*

We thank the reviewer for bringing this to our attention, we have now included the citation in the introduction.

> *"Hidden" in your title seems too much.*

We changed the title to more accurately describe our findings and removed 'hidden'.

> *While I'm glad you didn't record at room temperature, the choice of 30C seems a bit unfortunate - if you go to the trouble to heat the bath, why not at least 34C, which is reasonably standard as an approximation for physiological temperature?*

We thank the reviewer for pointing this out. The choice of 30C was made to approach physiological temperature levels, while preserving the slices for extended amounts of time which is a standard approach. Future experiments in vivo be performed to further understand the naturalistic relevance at ~37C.

> *Line 506: do you mean "Hz" here? It's not a frequency, is it? I think it's a unitless ratio?*

Correct, we have amended the typo.

> *Line 95: you have not shown that HCN is "essential" for "excess" AP firing.*

We have corrected the phrasing, we agree.

> *Fig. 2b,c: is this data from a single example neuron, maybe the same neuron as in 2a? Or from all recorded neurons pooled?*

The data is from several recorded cells pooled.

> *Fig. 3 (important figure):*
>
> *Why did you not use a paired test for panels e and f? You have the same number of neurons for each condition and the expectation is that you record each neuron in control and then in cesium condition, which would be a paired comparison. Or did you record only 1 condition per neuron?*
>
> *This figure presents your main finding (in my opinion). You should show examples of the synaptic responses, i.e. raw traces, for each condition and panel, and overlaid in such a way that the reader can immediately see the relevant comparison - it's worth the space it requires.*

We thank the reviewer for the suggestions. Traces are only overlaid in the paper when they come from the same cell. For Fig. 3d-i, EPSPs in every neuron were evoked in 2-3 different locations (i.e., 1-2 'L4' locations for Type-I and Type-II synapses, and one 'L1' location in each)

with the same stimulation pipette and one pharmacological condition per cell. Therefore two-sample t-test were used since the control and cesium conditions came from separate cells (i.e., separate observations). This was necessary, as we can never assume that the stimulating electrode can return back to the same synapse after moving it. We were not comfortable with showing overlaid traces from different cells, however, we did show representative traces from control and the Cs^+ conditions in Fig. 3h. Complementary ZD-7288 experiments can be found on panel b and c, *where we did perform within-cell pharmacology* (and thus used paired t-tests) from one stimulation area/cell. We hope these complementary experiments increase overall confidence as neither pharmacological approach is 100% without off-target effects. We now also included more overlaid traces where appropriate (i.e., Fig. 3b, and in the new Fig. 3k experiments using within-cell pharmacology comparisons). We do realize these complementary approaches could cause confusion to the reader, and have now done our best to make the slightly different approaches in this Figure clearer in the results section.

> *Consider repeating at least some of these critical experiments with ZD7288 instead of Cs+ (and not K-gluc), or even with ZD7288 pipette perfusion, if it's technically feasible here.*

We thank the reviewer for the suggestions. Although many of our recordings using Cs^+ already had complementary experiments (such as synaptic experiments Figure 3e vs Figure 3b), we recognize the need to extend the manuscript with more ZD-7288 experiments. We have now extended Figure 1 with three panels (Figure 1 c,d,e), which recapitulates a fundamental finding, the change in overall excitability upon HCN channel blockade, using ZD-7288 as well.

> *Fig. 3a, why show a schematic (and weirdly scaled) stimulating electrode? Don't you have a BF photo showing the actual stimulating electrode, which you could trace to scale or overlay? Could you use this panel to indicate what counts as "distal" and what as "proximal", visually?*

The stimulating electrode was unfortunately not filled with florescent materials, therefore it was not captured during the z-stack.

> *Fig. 3b: is the y-axis labeled correctly? A "100% change" would mean a doubling, but based on the data points here I think y=100% means "no change"?*

The scale is labeled correctly, 100% means doubling.

> *Fig. 3b, c: again, show traces representing distal and proximal, not just one example (without telling us how far it was). And use those traces to illustrate the half-width measurement, which may be non-trivial.*

We have extended Figure 3b with an inset showing the effect of ZD-7288 on a proximal stimulating site. The legend now includes additional information indicating stimulating location 28 µm away from the soma in control conditions (black trace) and upon Z-7288 application (green trace).

> *Line 543, 549: it seems you swapped labels "h" and "i"?*

Typo corrected.

> *Fig. 4b: to me, MK-801 only *partially* blocks amplification, but in the text L198 you write "abolish".*

We thank the reviewer for pointing this out. Indeed, there are several other subthreshold mechanisms that are still intact after pipette perfusion, which can cause amplification. We have now clarified this in the text (p7).

> *Fig. 4e,f: what is the message? Uniform NMDAR? The red asterisk in (e) is at a proximal/distal ratio of roughly 1. I don't understand the meaning of the asterisk (the legend is too basic) and I'm surprised to see a ratio of 1 as the best fit, and also that the red asterisk is at a dendritic distance of 0 um in (f). This could use more explanation (if you feel it's relevant).*

We thank the reviewer for pointing this out. We have now included a better explanation in the results and figure legend. We have also updated the figure to make it clearer and added model traces in Fig. 4f, which correspond to example data from slices in Fig. 4g (both green). The graph suggests nonuniform, proximally abundant NMDA distribution. The color coding corresponds to the proximal EPSP halfwidth divided by distal EPSP halfwidth. It is true that the dendritic distance 'center' was best-fit very close to the soma, but also note the dispersion (distribution) half-width was >150mm, so there is quite a significant dendritic spread despite the proximal bias prediction. Based on this model there is likely NMDA spread throughout the entire dendrite, but biased proximally. Naturally, future work will need to map this at the spine level so this is currently an oversimplification. Nonetheless, a proximal NMDA bias was necessary to recapitulate findings from Fig. 3, and additional slice recordings in Fig. 4 were consistent with this interpretation.

> *Fig. 4g: I feel your choice of which traces to overlay is focusing on the wrong question. As the reader, what I want to see here is an overlay of all 4 conditions for one pathway. If this is a sequential recording in a single cell (Cs, Cs+MK801, wash out Cs, MK801), then the overlay would be ideal and need not be scaled. Otherwise, you can scale it. But the L1/L4 comparison does not seem appropriate to me. I find myself trying to imagine what all the dark lines would look like overlaid, and all the light lines overlaid separately. Also, the time axis is missing from this panel. Consider a subtraction of traces (if appropriate).*

In these recordings, all EPSPs cells were measured using a stimulating electrode that was moved between L1 and L4 (only once, to keep the exact input consistent) to measure the different inputs in a single neuron. In separate sets of experiments, the same method was used but in the presence of Cs^+, Cs^+ + MK-801, or MK-801 alone. This was the most controlled method in our hands for this type of approach, as drug wash outs were either impractical or not possible. Overlaying four traces would have presented a more cluttered image, and were not actually performed experimentally. As our aim was to resolve the proximal-distal halfwidth relationship, therefore we deemed the within-cell L1 vs. L4 comparison appropriate. We have nonetheless added model traces in Fig. 4f, which correspond to example data from slices in Fig. 4g (both green). The bar graphs should serve also serve to illustrate the input-specific relationship- i.e., that the only time the L1 and L4 EPSP relationship was inverted was in the presence of Cs^+ (green bars) and that this effect was occluded with simultaneous MK-801 in the pipette (red bars).

> *Line 579: should "hyperpolarized" be depolarized?*

Corrected

> *Fig. 5a: it looks like the HCN density is high in the most basal dendrites (black curve above), then drops towards the soma, then rises again in the apicals (red curve). Is that indeed how the density was modeled? If so, this is completely at odds with the impression I received from reading your text and experimental data - there, "proximal" seems to*

> *mean where the L4 axons are, and "distal" seems to mean where the L1 axons are, in other words, high HCN towards the pia and low HCN towards the white matter. But this diagram suggests a biphasic hill-valley-hill distribution of HCN (meaning there is a second "distal" region below the soma). In that case, would the laterally-distant basal dendrites also be considered distal? How does the model implement the distribution - is it 1D, 2D or 3D? As you can probably tell, this figure raised more questions for me and made me wonder why I don't have a better understanding yet of your definitions.*

We thank the reviewer for pointing this out. We agree our initial cartoon of the parameter fitting procedure was not accurate and should have just been depicted a single 'curve'. We have now simplified it to better demonstrate what the model is testing, and also made the terms more consistent and accurate. There is no 'second' region in the model. We hope this better illustrates it now. We also edited the legend to be clearer. Because the model description in Fig. 4d suffered from similar shortcomings, we also modified it accordingly as well as the figure legend there.

> *Fig. 5b: why is the best fit at a proximal/distal ratio of 1, yet sigma is 50 um?*

Proximal/distal bias on this figure was fitted to 0.985 (prox/distal ratio) as we modeled control conditions, with intact NDMA and HCN channels, which closely approximated the control recording comparisons.

> *Fig. 6h, Line 662: "vs CsMeSO4 … for putative LGN events" The panel shows proximal vs distal, not control vs Cs+. What's going on here?*

Typo corrected.

> *Fig. 7e: the ctrl sag ratio here averages 0.02, while in Fig. S1 the average (for V1 and others) is about 0.07. Please refer to our answer given to the previous question regarding sag ratio measurements. Briefly, recordings made with 5-CT application were made using a less severe, -2 pA/pF current injection to test seg responses. This more modest hyperpolarization activated less HCN channels, therefore the sag ratio is lower compared to previously reported datapoints.*

We have included this explanation in the methods section (page 14)

> *Now hear you are using a paired test for this pharmacology, but you didn't previously (see my earlier comments/questions).*

Paired t-test were used for these experiments as these control and test datapoints came from the same cell. Cells were recorded in control conditions, and after drug application.

> *Line 137: single-axon activation: but cortical axons make multi-synaptic contacts, at least for certain types of pre- and post-synaptic neurons, and (e.g. in L5-L5 pairs) those contacts can be distributed across the entire dendritic arbor. In other words, it's possible that when you stimulate in L1, you activate local axons, and the signal could then propagate to multiple synaptic contact locations, some being distal and some proximal. Maybe you have reasons to believe you're able to avoid this?*

We thank the reviewer for this question. Cortical axons often make distributed contacts, however, top-down and bottom-up pathways innervating L2/3 PCs are at least somewhat restricted to L2/3/L4 and L1, respectively (Shen et al. 2022, Sermet et al. 2019). Therefore, due to the lack evidence suggesting a heavily mixed topographical distribution for top-down and bottom-up inputs, we have reason to believe that L1 stimulation will result in mainly distal

input recruitment, while L4 stimulation will mainly excite proximal dendritic regions. The resolution of our experiments was also improved by the minimal stimulation and visual guidance (subset of experiments) of the stimulation. Furthermore, new optogenetic experiments stimulating LGN and LM axons, which have been anatomically defined previously as biased to deeper layers and L1, respectively, were now also performed (Fig. 3j-l) with analogous cesium effects as our local electrical stimulation experiments. Future work using varying optogenetic stimulation parameters will expand on this.

> *L140: "previous reports" ==> citation needed.*

We have inserted the citation needed.

> *L149: "arriving to layer 1"; but I think earlier you noted that some or many L2/3 neurons lack a dendritic tuft; do they all nevertheless have dendrites in L1? Note that cortico-cortical long-range axons still need to pass through all cortical layers on their way up to L1.*

We thank the reviewer for the question. Although the more superficial L2/3 PCs lack distinct apical tuft, their dendrites reach the pia similarly to deeper L2/3 PCs. All of our recorded and post-hoc recovered cells had dendrites in L1, except in cases where they were clearly cut during the slicing procedure, which cells were occluded from the study.

> *When you write "L4 axons" or "L4 inputs", do you specifically mean long-range thalamic axons? Or axons from local L4 neurons? What about axons in L4 that originate from L5 pyramidal neurons?*

In case of 'L4' axons, we cannot disambiguate these inputs *a priori*, as they are both part of the bottom-up pathway, and are possibly experimentally indistinguishable. Even with restricted opto LGN stimulation, disynaptic inputs via L4 PCs cannot be completely ruled out under our conditions. On the other hand, the probability of L5 PC axons to terminate on L2/3 PCs is exceedingly low (single reported connection out of 1145 potential connections; Hage et al. 2022). We did find two clearly different synaptic subpopulations (Supp. Fig 3) in L4- which was tempting to classify as one or the other. However we felt there was not enough evidence in the literature as well as our additional optogenetic experiments to make a classification on the source of these different L4 inputs. Thus we deemed them as Type-I or Type-II for now.

> *Do you inject more holding current to compensate for the resting membrane potential when Cs+ or ZD7288 is in the bath?*

We thank the reviewer for the question. We did not inject a compensatory current, as we wanted to investigate the dual, physiologically relevant action of HCN channels (George et al. 2009)

> *I'd like to see distributions (histograms) of L4 and L1 EPSP amplitudes, under control conditions and ideally also under HCN block.*

We have now extended the manuscript with a supplementary figure (Supplementary Figure 6) to show that EPSP peak was not distance dependent in control conditions, and there was no relationship between peak and halfwidth in our dataset.

> *Line 186, custom pipette perfusion: why not use this for internal ZD7288, to make it cell-specific?*

We thank the reviewer for the question, this is a good point. In future work we will consider this when applicable. It is certainly a way to control for bath application confounds in many ways.

> *L205: "recapitulate our experimental findings" - which findings do you mean? I think a bit of explanation/referencing would help.*

Corrected.

> *Line 210: L4-evoked were narrower than L1-evoked: is this not expected based on filtering?*

We thank the reviewer for pointing this out, the word “Intriguingly” has been omitted.

> *Line 231 and 235: "in L5 PCs" should be restricted to L5 PT-type PCs.*

We have corrected this throughout the manuscript.

> *Neuromodulation, Fig. 7, L263-282: the neuromodulation finding is interesting. However, a bit like the developmental figure, it feels "tacked on" and the transition feels a bit awkward. I think you may want to discuss/cite more of the existing literature on neuromodulatory interactions with HCN (not just L2/3). Most importantly, what I feel is missing is a connection to your main finding, namely L1 and L4 inputs. Does serotonergic neuromodulation put L1 and L4 back on equal footing, or does it exaggerate the differences?*

We thank the reviewer for the question. We agree with the reviewer that Figure 7 does not give a complete picture about how the adult brain can capitalize on this channel distribution, as our intention was to show that HCN channels are not a stationary feature of L2/3 PC, but a feature which can be regulated developmentally and even in the adult brain via neuromodulation. In other words, the subthreshold NMDA boosting we observed can be gated by HCN, depending on developmental stage and/or neuromodulatory state of the system. We have now added some brief language to better introduce the transition and its relevance to the current study in the results (p8), and discussed the implications in the discussion section of the original manuscript.

> *General comment: different types/sources of synapses may have different EPSP kinetics. I feel this is not mentioned/discussed adequately, considering your emphasis on EPSPs/HCN.*

See points above on input-specific synaptic diversity.

> *Line 319/320: enriched distal HCN is found in L5 PT-type, not in all L5 PCs.*

Corrected

> *L320: CA1 reportedly has a subset of pyramidal neurons that have higher proximal HCN than distal (I gave the citation above). In light of that, I think "unprecedented" is an overstatement.*

Corrected.

> *Methods:*

> *L367: What form of anesthesia was used?*

Amended.

> *Which brain areas, and how?*

Amended.

> *Why did you first hold slices at 34C, but during recording hold at 30C?*

We held the slices at 34C to accelerate the degradation of superficial damaged parts of the slice, which is in line with currently used acute slice preparation methodologies, regardless of the subsequent recording temperature.

> *Pipette resistance/tip size?*

Amended.

> *Cell-attached recordings (L385): provide details of recordings. What was the command potential (fixed value, or did you adjust it per neuron by some criteria)?*

Amended.

> *What type of stimulating electrode did you use? If glass, what solution is inside, and what tip size?*

We thank the reviewer for pointing these out, the specific points were added to the methods section.

> *L392/393: you adjusted the holding (bias) current to sit at -80 mV. What were the range and max values of holding current? Was -80 mV the "raw" potential, or did it account for liquid junction? If you did not account for liquid junction potential, then would -80 in your hands effectively be between -95 and -90 mV? That seems unusually hyperpolarized.*

All cells were held with bias holding currents between -50 pA and 150 pA. To be clear, as mentioned below, we did not change the bias current after any drug applications. We did not correct for liquid junction potential, and cells were ‘held‘ with bias current at -80 mV as during our recordings, as *1)* this value was apparently close to the RMP (i.e. little bias current needed at this voltage on average) (Fig. 2e) and *2)* to keep consistent conditions across recordings. The uncorrected -80 mV is in the range of previously reported membrane potential values both *in vivo* and *in vitro* (Svoboda et al. 1999, Oswald et al. 2008, Luo et al. 2017), which found the (corrected) RMP to be below -80mV. Naturally this will not reflect every *in vivo* condition completely and further investigation using naturalistic conditions in the future are warranted.

> *Did you adjust the bias current during/after pharmacology?*

Bias current was not adjusted in order to resolve the effect on resting membrane potential.

> *L398: sag calculation could use better explanation: how did you combine/analyze multiple steps from a single neuron when calculating sag? Did you choose one level (how) or did you average across step sizes or ...?*

Sag ratio was measured at -6 pA/pF current step except for one set of experiments in Fig. 7. Methods section was amended.

> *L400, 401: 10 uM Alexa-594 or 30 um Alexa-594, which is correct?*

10 μM is correct, typo was corrected

> *L445: "PV cell" seems like a typo?*

Typo is corrected.

> *L450: "altered", please describe the algorithm or manual process.*

Alterations were made manually.

> *L474: NDMA, typo.*

Typo is fixed.

> *L474: "were adjusted", again please describe the process.*

Adjustments were made by a grid-search algorithm.

> *Biel, M., Wahl-Schott, C., Michalakis, S., & Zong, X. (2009). Hyperpolarization-activated cation channels: from genes to function. Physiological reviews, 89(3), 847-885. https://journals.physiology.org/doi/full/10.1152/physrev.00029.2008 - (very comprehensive review of HCN)*
>
> *Bullis JB, Jones TD, Poolos NP. Reversed somatodendritic I(h) gradient in a class of rat hippocampal neurons with pyramidal morphology. J Physiol. 2007 Mar 1;579(Pt 2):431-43. doi: 10.1113/jphysiol.2006.123836. Epub 2006 Dec 21. PMID: 17185334; PMCID: PMC2075407. https://physoc.onlinelibrary.wiley.com/doi/full/10.1113/jphysiol.2006.123836 - (CA1 subset (PLPs) have a reversed HCN gradient; cell-attached patches, NMDAR)*
>
> *Velumian AA, Zhang L, Pennefather P, Carlen PL. Reversible inhibition of IK, IAHP, Ih, and ICa currents by internally applied gluconate in rat hippocampal pyramidal neurones. Pflugers Arch. 1997 Jan;433(3):343-50. doi: 10.1007/s004240050286. PMID: 9064651. https://link.springer.com/article/10.1007/s004240050286 - (K-Gluc internal inhibits HCN)*
>
> *Sheets, P. L., Suter, B. A., Kiritani, T., Chan, C. S., Surmeier, D. J., & Shepherd, G. M. (2011). Corticospinal-specific HCN expression in mouse motor cortex: I h-dependent synaptic integration as a candidate microcircuit mechanism involved in motor control. Journal of neurophysiology, 106(5), 2216-2231. https://journals.physiology.org/doi/full/10.1152/jn.00232.2011 - (L2/3 IT have same sag ratio as all other non-PT pyramidals, roughly 5% (vs 20% PT); intracellular ZD7288 used at 10 or 25 um)*
>
> *Harris NC, Constanti A. Mechanism of block by ZD 7288 of the hyperpolarization-activated inward rectifying current in guinea pig substantia nigra neurons in vitro. J Neurophysiol. 1995 Dec;74(6):2366-78. doi: 10.1152/jn.1995.74.6.2366. PMID: 8747199. https://journals.physiology.org/doi/abs/10.1152/jn.1995.74.6.2366 - (comparison Cs+ and ZD7288)*
>
> *Harris, N. C., Libri, V., & Constanti, A. (1994). Selective blockade of the hyperpolarization-activated cationic current (Ih) in guinea pig substantia nigra pars compacta neurones by*

a novel bradycardic agent, Zeneca ZM 227189. Neuroscience letters, 176(2), 221-225. https://www.sciencedirect.com/science/article/abs/pii/0304394094900876 - (Cs+ is not HCN-selective; it also broadens APs, reduces the AHP)

Chevaleyre, V., & Castillo, P. E. (2002). Assessing the role of Ih channels in synaptic transmission and mossy fiber LTP. Proceedings of the National Academy of Sciences, 99(14), 9538-9543. https://pnas.org/doi/abs/10.1073/pnas.142213199 - (Cs+ blocks K channels, increases transmitter release; but also ZD7288 affects synaptic transmission)

Thank you

https://doi.org/10.7554/eLife.96002.2.sa0